Biosensors and Bioelectronics 126 (2019) 68–81

Contents lists available at ScienceDirect

Biosensors and Bioelectronics

journal homepage: www.elsevier.com/locate/bios

Recent advances in microfluidic paper-based electrochemiluminescence analytical devices for point-of-care testing applications

Somasekhar R. Chinnadayyala[a,b], Jinsoo Park[a,b], Hien Thi Ngoc Le[c], Mallesh Santhosh[d], Abhijit N. Kadam[e], Sungbo Cho[b,c,*]

[a] Department of Biomedical Engineering, Gachon University, Incheon 21936, Republic of Korea
[b] Gachon Advanced Institute for Health Science & Technology, Gachon University, Incheon 21999, Republic of Korea
[c] Department of Electronic Engineering, Gachon University, 1342 Seongnamdaero, Sujeong-gu, Seongnam-si, Gyeonggi-do 13120, Republic of Korea
[d] Center of Integrated Biotechnology, Sogang University, 35 Baekbeom-ro, Sinsu-dong, Mapo-gu, Seoul, Republic of Korea
[e] Department of Chemical and Biological Engineering, Gachon University, 1342 Seongnamdaero, Sujeong-gu, Seongnam-si, Gyeonggi-do 13120, Republic of Korea

ARTICLE INFO

Keywords:
Cellulose paper
Screen printing
DNA
Biosensor
Tumor cells
Cytodevice
Rechargeable batteries

ABSTRACT

Electrogenerated chemiluminescence (ECL) is an effective method for detecting a wide range of analytes including metal ions, virulent DNA, pathogenic bacteria, tumor cells and glucose. The attractive features of paper including passive liquid transport and biocompatibility are the main two advantages of using paper as a biosensing platform. To achieve key factors in paper-based sensors, the fabrication procedures and the analysis methods are fine tuned to satisfy the requirements of the ultimate–users. Here, we review various ECL signal amplification labels, inexpensive and portable devices, such as rechargeable batteries, which have replaced traditional instrumentation and different light detection technologies used in paper ECL devices. We also highlight the current trends and developments in ECL paper-based microfluidic analytical devices, as well as recent applications of ECL–based detection methods and inexpensive microfluidic devices. We discuss various paper-based devices, including 3D-origami devices, and devices utilizing self-powered and bipolar electrodes. Significant efforts have also been dedicated towards paper based multiplexing analysis (multi-label, and the multi-analyte strategies) and integration of microfluidic lab-on-paper devices with competences for point-to-care diagnostics. This review finally tabulates systematized data on figures of merit and novel types of ECL labels, used for detection of various biomarkers and analytes.

1. Introduction

Electrochemiluminescence (ECL), or electrogenerated chemiluminescence, is a process of light emission in which species generated at the electrode surface undergo an exergonic electron-transfer reaction to form excited states that emit light (Bertoncello and Ugo, 2017; Rizwan et al., 2018). An ECL signal is produced via bimolecular recombination of electrogenerated radicals at the electrode surface. The mechanism of ECL is classified into two types, according to the source of radicals: the annihilation pathway and the co-reactant pathway. In the annihilation pathway, radical species are generated from a single emitter; in the co-reactant pathway, radical species are generated from a bimolecular set of electrochemical reactions between the emitter and a suitable co-reactant. The emitter plays a significant role in transformation of electrical energy into radiative energy. In most recent studies, three types of luminophores, including ruthenium(II) complexes, luminol, and quantum dots (QDs), are mainly used as ECL luminophores (Li et al., 2017a).

Combining chemiluminescence (CL) and electrochemistry in ECL is advantageous because it can increase sensitivity and widen the dynamic range inherited from conventional chemiluminescence, while preserving the simplicity, stability, and facility of the device (Zhou et al., 2015). ECL exhibits superior temporal and spatial control of light emission compared with other light-emission techniques such as photoluminescence (PL) and CL. In ECL, the absence of excitation light facilitates nearly zero background noise, whereas PL suffers from photoexcitation-induced background noise (Xu et al., 2016). For these reasons, ECL has become a powerful analytical technique used widely in numerous fields including immunoassays, bioanalysis, fundamental studies, food and environmental monitoring, and detection of trace

* Corresponding author at: Department of Electronic Engineering Gachon University, 1342 Seongnamdaero, Sujeong-gu, Seongnam-si, Gyeonggi-do 13120, Republic of Korea.
E-mail address: sbcho@gachon.ac.kr (S. Cho).

https://doi.org/10.1016/j.bios.2018.10.038
Received 25 July 2018; Received in revised form 6 October 2018; Accepted 18 October 2018
Available online 22 October 2018
0956-5663/

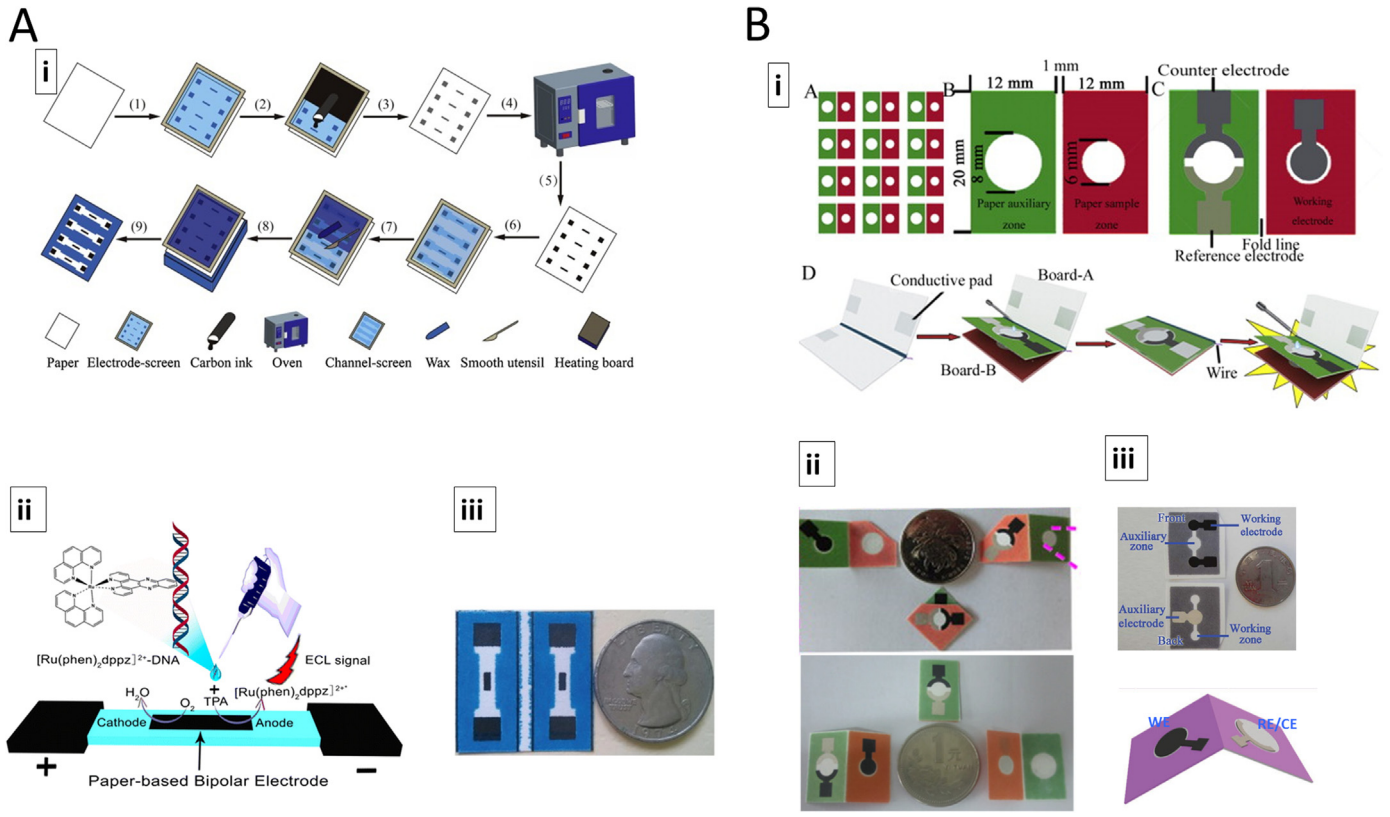

Fig. 1. Schematic representation of the screen-printing fabrication for the planar paper based BPE-ECL device (Chen et al., 2016) and origami paper based devices (Li et al., 2014a) (A-i and B-i). General configuration of the planar BPE-ECL device showing the driving electrodes and conducting BPE band (A-ii and A-iii). Three-electrode configuration of origami paper-based ECL system. The RE and CE were screen-printed on the same paper pad, whereas the WE(s) was (or were) screen-printed on another paper pad. Two-electrode configuration of origami paper-based ECL system in battery triggered ECL detections (B-ii and B-iii).

amounts of target molecules (Miao, 2008; Deng and Ju, 2013; Bertoncello et al., 2014). In the past decade, microfluidic paper-based analytical devices (μPADs) have been developed as a promising platform for point-of-care testing applications; paper is readily available, inexpensive, and is chemically compatible with many applications (Sia and Kricka, 2008; Mukhopadhyay, 2009; Martinez et al., 2010). μPADs have many advantages including inexpensive production on a mass scale (Apilux et al., 2010; deAraujo and Paixao, 2014; LaGasse et al., 2014). μPADs can be used to quantify various analytes in aqueous solutions and biological fluids such as urine, serum, and blood; they can also be used for multiplex analysis, are simple to operate, and can function without any external source (Nie et al., 2010).

Establishing ECL on μPADs, achieved by integrating μPADs and screen-printed electrodes, has increased the scope of ECL-based detection on μPADs and showed an excellent prospective for analyte detection in trace amounts (Yan et al., 2012a). Today, paper-based analytical devices, particularly micro paper-based ECL devices (μ-PECLD), have garnered considerable interest for their ability to improve health care in advanced and advancing societies (Cummins et al., 2016; Ge et al., 2014a, 2014b). In this context, point-of-care testing devices, integrated with paper microfluidics and ECL, play a key role in rapid diagnosis, prevention, and treatment of human diseases (Gross et al., 2017). Glucometers, used for the management of diabetes, and home pregnancy dipsticks, are the most popular examples of point-of-care testing (POCT) devices. However, the recently developed microfluidics integrated with smaller ECL sensors (Cummins et al., 2016) have broadened the range of application for POC diagnostics. Excellent reviews of POCT devices for use in global health have been published. The readers are requested to refer to (Chin et al., 2011; Yager et al., 2008) for a broad-scope review of this research area. For the general principles of mechanisms and functionalization chemistries used in the fabrication of μPADs, we recommend the readers consult the excellent reviews published in the literature (Martinez et al., 2010; Sher et al., 2017; Akyazi et al., 2018).

This review focuses on developments in paper-based ECL assays made from 2011 to 2018. Numerous reports on this subject have been published during the past 5 years, necessitating a comprehensive review. The aim of this review is to outline new advances in areas such as labeling agents and immobilization supports for paper-based ECL sensors, electrical energy supply devices and light detection technologies for paper-based ECL sensors, and representative ECL sensing applications. In conclusion, prospects for the development of ECL analysis will be discussed. Recent years have seen an explosion of publications in this active area of research. Therefore, it is impossible to cover all the work published in the past 8 years; however, we aimed to be as comprehensive as possible.

2. Labeling agents for paper-based ECL sensors

Most of the ECL luminophores display limited water solubility and stability during electrochemical reactions (Valenti et al., 2012). It is also difficult to introduce binding sites without affecting the electrochemical properties of these luminophores (Richter, 2004). These limitations restrict usage. Currently, the $Ru(bpy)_3^{2+}$ are the only luminophores employed in commercial applications of ECL (Bard, 2004). The broad emission bands of luminophores can be disadvantageous in biosensor applications where a multianalyte determination is desired. Paper-based ECL immunoassays play an important role in detecting low concentrations of analytes; therefore, achieving sufficient sensitivity, such as when detecting concentrations as low as pM in nL volumes, remains a challenge. Signal amplification strategies are used to amplify immunological interactions, thereby enhancing the response of paper-

based ECL sensors. Rapid developments in nanotechnology (Bertoncello and Forster, 2009; Pei et al., 2013) have produced high-performance paper-based ECL sensors because nanomaterials can act as: (a) a platform to increase the loading capacity of ECL labels; (b) an energy acceptor to quench the ECL; (c) a novel label for ECL detection; (d) an electrocatalyst in ECL reactions; (e) a promoter to improve electron transfer at the electrode interface and electrocatalytic activities. The nanomaterials and inorganic complexes used as labeling agents for paper-based analytical devices was represented as schematic in Fig. 1.

2.1. Semiconductor nanocrystals (QDs) as labels

Semiconducting nanocrystals or quantum dots (QDs), a class of unique nanomaterials with attractive optoelectronic properties, are used in diverse applications ranging from energy conversion systems to electronics and diagnostics (Amelia et al., 2012). In QDs, the ECL process involves high-energy electron transfer reactions with formation of excited species. These excited species emit light via two distinct means: (i) annihilation and (ii) co-reactant mechanisms. In the last two decades, the number of works on QDs in chemistry and bioanalysis have increased dramatically (Chan and Nie, 1998; Bruchez et al., 1998). However, a breakthrough in bioanalysis using QD-based ECLs was reported by Liu et al. (2007). Since then, QDs have gradually become one of the most common ECL luminophore-using immunoassays (Esteve-Turrillas and Abad-Fuentes, 2013). QDs are novel ECL luminophores displays a very high quantum yield, broad excitation spectrum, narrow and size-tunable luminescence spectrum and high resistivity towards photo bleaching These properties are attractive in paper-based ECL immunosensing. Herein, we focus on some of the most recent applications of QDs in microfluidic paper-based ECL biosensors.

Li et al. (2013a) synthesized water soluble QDs functionalized with nonporous silver (QDs/NPS) as the signal amplification label for highly sensitive ECL detection of carcinoembryonic antigen (CEA). Water-soluble CdTe QDs were synthesized using MPA as stabilizing agent according to a method of Deng et al. (2010). CdTe QDs, loaded onto nonporous silver (QDs/NPs), were attached on the surface of Ag-PWE using a sandwich immunoreaction. Signal amplification, generated by the high loading of CdTe QDs, resulted in highly sensitive detection of CEA with a good linear range and detection limit. The same research group developed a 3D origami multiple ECL immunodevice for α-fetoprotein (AFP). This device uses Ag-PWE as a sensing platform, multi-labeled nonporous gold–carbon spheres as tracers, and CdTe QDs and glucose oxidase (GOx) as labels. The possible mechanisms for CdTe QDs functioning as ECL labels in a QDs-H_2O_2 system are listed as follows:

$$QDs + e\text{-} \rightarrow QDs^{-\bullet} \quad (1)$$

$$Glucose + O_2 \xrightarrow{GOx} Gluconic\ acid + H_2O_2 \quad (2)$$

$$H_2O_2 + QDs^{-\bullet} \xrightarrow{Ag-PWE} QDs^{*} + products \quad (3)$$

$$QDs^{*} \rightarrow QDs + h\nu \quad (4)$$

Li et al. (2013c) synthesized carbon nanodots (CNDs) for a high throughput sandwich ECL immunoreaction to detect multiple cancer biomarkers using a potential resolution strategy. In the presence of $K_2S_2O_8$ as co-reactant, ECL intensity of nanoprobe (CNDs) increased with an increase in analyte concentration.

2.2. Carbon nanocrystals, graphene quantum dots and carbon dots as ECL labels

In general, semiconductor quantum dots (QDs), such as CdTe QDs, can release Cd^{2+} ions; these are a potential environmental hazard, causing cytotoxicity and limiting the application of QDs (Derfus et al., 2004). Fluorescent Carbon nanocrystals (CNCs), which have low toxicity, are prepared by electrochemical oxidation of graphite in an aqueous solution. Water-soluble CNCs generate ECL signals and provide abundant -COOH groups at surfaces, which is beneficial for ECL labeling (Zheng et al., 2009). In addition to low cytotoxicity, CNCs and are less costly and possess numerous advantages including ease of labeling, chemical inertness, lack of blinking, large two-photon excitation cross-sections, and a good biocompatibility compared with QDs that contain heavy metals. An ECL DNA sensor that employs CNC-coated silica nanoparticles (Si@CNCs) as labels based on functionalized DNA probes has been developed in a 3D μPAD for the detection of Pb^{2+} (Zhang et al., 2013a). The main advantages of this sensor can be attributed to two factors. First, a novel ECL label, generated using Si@CNC composites, shows excellent ECL activity. The silica nanoparticles, possessing an excellent monodispersity and uniform structure, are used as carriers for high loading of CNCs, which play a crucial role in enhancement of the ECL signal. Second, the wax-patterned 3D paper-based ECL device can provide fast, cost-effective, simple, and sensitive ECL detection.

Graphene quantum dots (GQDs) are emerging carbon-based materials made with graphene sheets smaller than 100 nm (Ponomarenko et al., 2008). GQDs exhibit new phenomena resulting from quantum confinement and edge effects. GQDs have attracted considerable attention and may gradually replace traditional semiconductor QDs because of their chemical inertness, low toxicity, biocompatibility, high fluorescence, and excellent photostability (Jia et al., 2017; Sun et al., 2013). Zhang et al. (2015) prepared water-soluble nitrogen-doped graphene quantum dots (N-QDs) using a facile one-pot solvothermal method by exfoliation and disintegration of graphite oxide. The N-GQDs are good ECL labels because of their low anodic ECL potential of + 0.84 V and high biocompatibility, which can facilitate highly sensitive ECL bioassays. An ultrasensitive paper-based ECL immunoassay was developed using green luminescent N-GQDs as ECL labels and AFP as model protein. A working paper electrode was fabricated using a seed-mediated growth approach in a promising platform for capturing antibodies. An ECL emission with a wide dynamic range occurs upon immunorecognition of the immobilized AFP by its antibody, labeled with N-GQDs, in the presence of 2-(dibutylamino)ethanol (DBAE) as co-reactant. The possible ECL mechanisms of the N-QDs-DBAE system are listed as follows:

$$N\text{-}GQDs \rightarrow N\text{-}GQDs^{\bullet +} + e- \quad (5)$$

$$DBAE \rightarrow DBAE^{\bullet +} + e- \quad (6)$$

$$DBAE^{\bullet +} \rightarrow DBAE^{\bullet} + H+ \quad (7)$$

$$N\text{-}GQDs^{\bullet +} + DBAE^{\bullet} \rightarrow N\text{-}GQDs^{*} + DBAE\ fragments \quad (8)$$

$$N\text{-}GQDs^{*} \rightarrow N\text{-}GQDs + h\nu \quad (9)$$

Green-luminescent GQDs functionalized with Au@Pt core-shell nanoparticles (GQDs/Au@Pt) were synthesized as signal labels for the sensitive point-of-care testing of CEA (Li et al., 2014a). An ECL nanoprobe (Ab_2/GQDs/Au@Pt) was designed by covalently assembling the signal antibody (Ab_2) on GQDs tagged with Au@Pt core-shell nanoparticles. After a sandwich-type immunoreaction, the GQDs/Au@Pt labels are captured onto the working electrode surface, which is composed of paper modified with nanoporous gold/chitosan. ECL signal amplification is achieved by catalysis of GOx and oxidation of glucose in situ. This generates H_2O_2 as coreactant and enhances Au@Pt in the ECL reaction of GQDs-H_2O_2. The possible ECL mechanisms are listed as follows:

$$Glucose + O_2 \xrightarrow{GOx} Gluconic\ acid + H_2O_2 \quad (10)$$

$$GQDs - e^{-} \rightarrow GQDs^{\bullet +} \quad (11)$$

$$H_2O_2 \Leftrightarrow H^{+} + HOO^{-} \quad (12)$$

$$HOO^- - e^{\bullet -} \rightarrow HOO^{\bullet} \leftrightarrow O_2^{\bullet -} \quad (13)$$

$$GQDs^{\bullet +} + O_2^{\bullet -} \rightarrow GQDs^* \quad (14)$$

$$GQDs^* \rightarrow GQDs + h\nu \quad (15)$$

Biocompatible ECL-emitting species and co-reactants have garnered more attention recently in the development of ECL sensors. Photoluminescent carbon-dots provide exciting opportunities for the development of biocompatible ECL nanolabels. Carbon dots (C-dots) are important in the nano-carbon family because of their benign and abundant nature (Baker and Baker, 2010). C-dots are better ECL nanolabels than semiconductor nanocrystal quantum dots. The physicochemical properties of C-dots are similar to those of semiconductor nanocrystal quantum dots; however, C-dots are less costly and exhibit low cytotoxicity, excellent biocompatibility, and good solubility in water (Wang et al., 2011; Du et al., 2013).

Wu et al. (2016) has developed a paper-based ECL cytodevice using PtNi@carbon dots-ConA as nanolabels for the detection of cancer cells and in-situ screening of anticancer drugs. A PtNi alloy, with bicontinuous and controllable network architecture, was used as support for loading C-dots. PtNi@C-dot-ConA bioconjugates participate in the ECL reaction of $K_2S_2O_8$ in Au@Pd-PWE to produce a quantitative ECL emission peak. The ECL response is based on the electron transfer between the reduced species formed in the PtNi@C-dot and the oxidized species of the co-reactant ($S_2O_8^{2-}$). The possible mechanisms of the PtNi@C-dot-S2O8^{2-} ECL processes are listed as follows:

$$S_2O_8^{2-} + e^- \rightarrow SO_4^{\bullet -} + SO_4^{2-} \quad (16)$$

$$PtNi@C-dot + e^- \rightarrow PtNi@C-dot^{\bullet -} \quad (17)$$

$$PtNi@C-dot^{\bullet -} + SO4^{\bullet -} \rightarrow PtNi@C-dot^{\bullet} + SO4^{2-} \quad (18)$$

$$PtNi@C-dot^{\bullet} \rightarrow PtNi@C-dot + h\nu \quad (19)$$

Using pyrolysis of citric acid, Liu et al. (2014) developed a one-pot synthetic strategy for the preparation of high quantum yield blue luminescent C-dots; these are used for the sensitive detection of cancer antigen 125. These C-dots are loaded onto amino-functionalized mesoporous silica nanoparticles, which act as amplification labels on a silver nanoparticle-coated paper working electrode (Ag-PWE). Wu et al. (2015b) developed oligonucleotide-functionalized CDs for the sensitive ECL detection of the IgG antigen using the rolling-circle amplification (RCA) technique. These CDs were synthesized from a graphite rod working electrode by electro-oxidation at 3 V against an Ag/AgCl reference electrode, with a Pt mesh in Phosphate buffer saline (PBS) used as a counter electrode.

2.3. Metallic nanoparticles as ECL labels

Nanoparticles with unique physical and electrical properties are widely used in immunosensing devices for the sensitive detection of various analytes. Due to their large surface area to volume ratio, long-term stability, easily controllable size distribution, high conductivity, and facile biomolecular conjugation, NPs are employed in different bioaffinity assays. Nanoporous materials have attracted considerable attention in recent years due to their high in-plane conductivity, good stability and biocompatibility.

Yan et al. (2014) synthesized nanotubular mesoporous Pt–Ag alloy nanoparticles, modified with a phenyleneethynylene derivative, as ECL nanolabels for highly sensitive determination of CEA in human serum samples. As novel ECL signal amplifiers, nanotubular mesoporous Pt–Ag alloy nanoparticles (P-acid/Pt–AgANPs) modified with phenyleneethynylene derivatives (4,4-(2,5-dimethoxy-1,4-phenylene) bis (ethyne-2,1- diyl)dibenzoic acid; P-acid) provide hollow porous nanostructures that have highly accessible surface areas and rich surface chemistry. This allows for vast functionalization of P-acid, resulting in ultrasensitive and multi-labeling signal amplification. The preparation of P-acid/Pt–AgANPs labels has been described previously (Lu et al., 2012). The mechanisms driving ECL reactions, involving gold/graphene/WE immobilized with sandwich immunocomplexes and labeled with P-acid/Pt–AgANPs in the presence of TPA, are listed as follows:

$$P-acid - e^- \rightarrow P-acid^{\bullet +} \quad (20)$$

$$TPrA - e^- \rightarrow [TPrA^{\bullet}]^+ \rightarrow TPrA^{\bullet} + H^+ \quad (21)$$

$$P-acid^{\bullet +} + TPrA^{\bullet} \rightarrow P\text{-}acid^* + products \quad (22)$$

$$P-acid^* \rightarrow P\text{-}^{acid} + h\nu \quad (23)$$

Li et al. (2013b) synthesized a novel label with ECL signal amplification for ultrasensitive detection of cancer markers using (P-acid)-functionalized nanoporous silver (P-acid/NPS). P-acid and NPS were synthesized as reported previously (Xu et al., 2011). NPS can form a coordination compound with -COOH groups; thereby, NPS can be directly conjugated with P-acid. The ECL responses of the Graphene oxide-chitosan/gold nanoparticles paper working zone, immobilized with sandwich immunocomplexes and labeled with P-acid/NPS in the presence of TPrA as co-reactant, were assessed using scanning/constant-potential. Li et al. (2014c) synthesized Pd@Au NP-loaded GOx as a signal amplification label for the highly sensitive detection of cancer biomarkers. The Pd@Au NPs were prepared by wet-chemical synthesis according to a previously published protocol by Huang et al. (2013). The novel porous paper working electrode modified with flower-like Ag@Au hybrids (Ag@Au-PWE) was used as a sensor platform for attachment of Ab_1. The 3D immunodevice was incubated with a sample solution containing different concentrations of CA125 in PBS at room temperature. The Ab_2, labeled with Pd@Au NPs/GOD, was linked to the Ag@Au-PWE surface via sandwich immunoreactions. After washing with washing buffer, and using a simple home-made device-holder, the immunodevice was connected to an electrochemical workstation. A PBS solution, containing $K_2S_2O_8$ and glucose, was added to record the ECL responses in the detection of cancer biomarkers. The possible mechanisms of ECL emission via $K_2S_2O_8$ and H_2O_2 are listed as follows:

$$S_2O_8^{2-} + e^- \rightarrow SO4^{-\bullet} + SO_4^{2-} \quad (24)$$

$$SO_4^{-\bullet} + H_2O \rightarrow HO^{\bullet} + HSO^{4-} \quad (25)$$

$$HO^{\bullet} \rightarrow HOO^{\bullet} + H_2O \quad (26)$$

$$Glucose + O_2 \xrightarrow{GOx} Gluconic\ acid + H_2O_2 \quad (27)$$

$$H_2O_2 \xrightarrow{Pd@Au\ NPs} PO_2 + H_2O \quad (28)$$

$$O_2 + H_2O + e^- \rightarrow HOO^{\bullet} + HO^- \quad (29)$$

$$SO_4^{-\bullet} + HOO^{\bullet} \rightarrow HSO_4^- + {}^1(O2)_{2*} \quad (30)$$

$${}^1(O2)_2{}^* \rightarrow 2{}^3O_2 + h\nu \quad (31)$$

3. Fabrication strategies of ECL paper devices

Paper in fabrication of microfluidic devices can be broadly defined as 'any material in the form of a thin ($\leq$ 1 mm) and flexible sheet that wicks aqueous solutions by capillary action'. The aforesaid definition of paper includes thousands of commercially available materials, ranging from everyday paper towels to highly engineered polymer membranes with a wide variety of wicking rates, thicknesses, pore sizes, chemical compositions and costs. While selecting the paper to make a μPAD, one must consider the properties of the paper since they directly translated into the properties of the channels in the device. A detailed information on the selection of paper for μPADs is given in the Supplementary information.

μPADs were fabricated mainly by patterning and manipulation of the hydrophilic property of paper (Li et al., 2012). Patterning paper into

hydrophilic channels demarcate by hydrophobic barriers creates microfluidic devices which enables distribution of a sample into multiple, spatially segregated regions. In almost all cases, hydrophilic channels in μPADs are distinct by the presence of hydrophobic barriers based on photoresist (Zhang et al., 2013b), wax (Chen et al., 2016; Yang et al., 2017), polydimethylsiloxane (Han et al., 2013; Sardesai et al., 2013) alkylketene dimer (Delaney et al., 2011), polystyrene (Olkkonen et al., 2010), poly(o-nitrobenzyl methacrylate) (Haller et al., 2011), fluorochemicals (Glavan et al., 2013), methylsilsesquioxane (Wang et al., 2014a, 2014b), and toner (Shi et al., 2012). The hydrophobic barriers were fabricated primarily by using photolithography (Klasner et al., 2010; Kakoti et al., 2015), various printing methods that form hydrophobic barriers (Feng et al., 2015; Sun et al., 2018; Maejima et al., 2013), cutting (Glavan et al., 2013), and chemical vapor deposition (Haller et al., 2011). Each fabrication method has advantages and limitations.

In fabrication of ECL microfluidic devices, carbon-based working electrodes are usually screen-printed onto a cheap substrate such as paper, while metal electrodes (silver and gold) are usually deposited via deposition procedures and ink jet printing. A common electrode-based ECL sensing unit for microfluidic paper based devices is composed of three electrodes: a working electrode (WE), a counter electrode (CE), and a reference electrode (RE) (Fig. 1B; ii-iii) (Wang et al., 2012b; Wu et al., 2015a; Xu et al., 2016; Liu et al., 2016; Li et al., 2017b). A two-electrode ECL system (WE and CE), was usually used with a commercial battery (Wang et al., 2012a and 2012b, Li et al., 2013b), a primary battery (Zhang et al., 2013b) or a cell phone. The paper based ECL devices were fabricated in two configurations for POCT applications:

3.1. Planar BPE paper based devices

The integration of disposable paper-based platforms with ECL bipolar electrodes was first demonstrated by Chen's research group for sensitive ECL detection of prostate-specific antigen (Feng et al., 2014b). In a microfluidic device, the BPE paper consists of two hydrophilic channels patterned using hydrophobic barrier. These two hydrophilic channels are connected by a BPE as an electronic conductor. The BPE and driving electrodes (driving anode and driving cathode) were screen printed directly onto the inexpensive cellulose paper. The biochemical functionalities were usually carried out on cathodes and analytic solution could drop in sensing cell (cathodic pole) and co-reactant solution in the reporting cell (anodic pole) (Fig. 1A; ii-iii). Due to the electronic conduction between cathode and anode, the electron transfer processes occurs at the BPE are coupled electronically to the ECL reaction, permitting the ECL light output to be quantitatively correlated to electrochemical reductions at the cathode. The fabrication steps of a general BPE prototype explained by Feng et al., includes: (a) cutting of the cellulose paper into specific dimensions (100 mm × 100 mm), (b) printing of electrode shapes and hydrophobic barrier on cellulose paper using Adobe illustrator, (c) carbon-ink screen printing of the electrodes (BPE and driving electrodes) onto the paper, (d) paper hydrophobization using wax to construct the hydrophobic barrier, (d) curing of the paper at specified time and temperature and subsequent placing of the paper to apply solid wax on to the paper, (e) melting of the wax into the paper by placing the wax screen printed paper along with screens onto the heating board (Fig. 1A; i). Advantages of BPE's include their inherent simplicity, easy fabrication, high sensitivity and ability to detect two analytes, one at each electrode pole, along with their “wireless” nature. These features facilitate their compatibility for ECL detection in microfluidic devices. The conventional BPE-ECL detection systems usually employ complicated and relatively expensive microfluidic technologies to integrate the detection cell into miniaturized lab-on-a-chip devices. Furthermore, these techniques require expensive instrumentation or skilled personnel, which limits their utility for point-of-care diagnostics.

3.2. 3D Origami paper based devices

Three dimensional paper microfluidic devices use inexpensive methods to integrate complex fluid networks and detection zones, such as electrochemical cells. These characteristics allow for applications such as point of care diagnostics. The 3D origami paper-based ECL devices were fabricated from a patterned pure cellulose paper cut into 2 pieces, designated as paper-A and paper-B. The fabrication steps of this 3D device involve: (a) Patterning of the hydrophilic working zones via Adobe Illustrator CS4 software; (b) bulk production of paper-A and paper-B, and wax pattering of the circular working zone; (c) baking of wax-patterned paper sheets in an oven at optimum temperature for specified time interval to melt the printed wax and enable it to penetrate through the paper; (d) screen printing/deposition of paper-A and paper-B hydrophilic zones with carbon ink/nanomaterials and Ag/AgCl to generate the working electrode, carbon counter electrode, and reference electrode respectively; the wax patterns around the paper-electrodes constitute a reservoir of electrochemical cells with specified volumes for paper-A and paper-B; (e) Integration of paper-electrodes with a newly designed device-holder to fix and connect the 3D paper-based ECL device containing Ag-conductive pads (Fig. 1B; i). The holder allows electrical contact and precise alignment of the electrodes and electrochemical cells. Many 3D devices fabrication is a time consuming process. They are fabricated layer-by-layer which does not allow for mass production of the devices. The layers are typically held together with double sided tape and holes are cut into the device with sophisticated tools like laser cutters. Three dimensional folded paper microfluidic devices (3D origami devices) reported by Yu's group (Zhang et al., 2013a; Wang et al., 2012b; Li et al., 2013c; Ge et al., 2012) and other groups group (Zhang et al., 2013b; Gu et al., 2014) with the goal of overcoming the complexities in 3D device fabrication. Folding of the paper excluded difficult alignment procedures and exact cuttings. The advantage of this configuration includes, bulk operations on or in working electrodes and a high integration (for multiplex assay) of working electrodes on cellulose paper, removing the need to consider the position and pattern of the reference and counter electrode.

4. Electrical energy supply devices for paper-based ECL sensors

Having a unique power supply is valuable when miniaturizing ECL devices for field operation and POCT. An electrochemical workstation is generally used in traditional ECL detection methods to initiate and control the luminescence. Due to the excessive costs of electrochemical workstations, significant efforts have been made to develop alternative power sources for ECL POCT. Low-cost and portable rechargeable batteries present one example. The advantages of rechargeable batteries include high efficiency, large capacity, low self-discharge rate, and output voltage stability. These factors render rechargeable batteries appropriate in fabrication of portable devices for POCT and on-site testing. Wang et al. (2013) developed battery-triggered (constant-potential) ECL detection of multiple tumor markers on a μ-PAD. A low-cost and simple voltage-controller was designed to precisely control the output voltage of the battery. Simultaneous determination of two analytes using one μ-PAD was achieved by controlling the operational constant-potential and by reversing the connection mode. Yang et al. (2014a, 2014b) used a low-cost, portable rechargeable battery as a power source, providing constant potential to pen-on-paper electrodes and triggering the ECL reactions. Chen et al. (2016) developed a handheld paper-based bipolar electrode-electrochemiluminescence (P-BPE-ECL) system using a rechargeable battery as a power supply and a smartphone to read the ECL signal. The quantitative ability of the P-BPE-ECL system was demonstrated using the luminol/H_2O_2-ECL system. To demonstrate the applicability of the P-BPE-ECL system, glucose was detected with a high limit of detection. Li et al. (2013b) coupled a low-cost voltage controller to a battery, allowing for tuning of the applied voltage. This device uses wax printing to define the

microfluidic channels and consists of two screen-printed carbon working electrodes modified to conduct immunoassays. A few alternative electrical energy supply devices in paper based ECL sensors were discussed in Supplementary information under section electrical energy supply devices for paper-based ECL sensors.

5. Light detection technologies for paper-based ECL sensors

The demand for portable, cost-effective, and user-friendly ECL detectors, with acceptable sensitivity for use in POCT devices, has given rise to alternative light sensors. Signal collection is one of the most important steps in ECL sensing systems. It is often accomplished using a PMT because of its higher sensitivity. Recently a couple of commercial ECL systems were used in paper based ECL studies (Flow injection luminescence analyzer- IFFM-E; multifunctional electrochemical and chemiluminescent analytical system- MPI-B; MPI-E; Ultra weak luminescence analyzer RFL-200) developed at the Changchun Institute of Applied Chemistry, Chinese Academy of Sciences, and manufactured by Xi'an Remex analytical instrument Ltd. Co., (Xi'an, China) (Li et al., 2014a, 2013b, 2017b; Zhang et al., 2015; Ge et al., 2012; Wang et al., 2013; Sun et al., 2018).

Charge coupled devices (CCDs), complementary metal oxide semiconductors, and silicon and organic photodiodes have recently been used as alternative light sources (Roda et al., 2016). In case of CCDs, modern cooled back-side illuminated CCDs are very popular and can reach a quantum efficiency of up to 90%, read-out noise of ≤ 5 e^-, dark count rates of 0.001 e^-/s, and formats as large as 4096×4096 pixels. While, Modern back-illuminated CMOS offer higher sensitivity, ensuring high signal-to-noise ratio even in low-light conditions, in which the entire area of each pixel is used for photon capture. Whereas, digital camera as light detector in paper-based ECL sensors can reduce the cost of measurement (Delaney et al., 2013; Doeven et al., 2015). Smart phones, with high imaging and computing capabilities, and open-source operation systems, are increasingly playing a role in healthcare (Ozcan, 2014) Because of their various advanced features, smartphones have emerged as a promising digital platform for the development of various novel bioanalytical devices. Moreover, smartphones are used for developing rapid, real-time, point-of-care monitoring, which can significantly simplify the design and reduce the cost of detection systems (Zhang and Liu, 2016). The MI 2SC smartphone produced by Beijing Xiaomi Science and Technology Co., Ltd. and samsung I8910 HD icon mobile phones are found to provide the highest sensitivity in case of paper ECL sensors (Delaney et al., 2011; Chen et al., 2016). The ubiquitous availability and portability of smartphones are advantageous in the development of portable ECL devices. CMOS imagers are the most commonly used image sensor applications in the recent days for mobile phones. The constant progresses in the backside-illuminated CMOS (BSI-CMOS) used in smartphone cameras have led to enhanced image quality, superior functionalities, and a compact size. In addition to the higher pixel numbers (up to 41 MP), newly developed CMOS architecture and multi-lens systems facilitate low noise and high quality image capture even in low light conditions, allowing smartphone cameras to be used for sensitive luminescence detection (Roda et al., 2014). The integration of ECL sensing elements into an "all-in-one device" is one attractive option. The development of portable ECL sensors greatly depends on advances in light-detection and analysis technologies. A few recent alternative light detection technologies in paper based ECL sensors were discussed in Supplementary information under section light detection technologies for paper-based ECL sensors.

6. ECL sensor applications

Integrating paper microfluidics with ECL detection was first reported by Delaney et al. (2011). Subsequently, various bio-affinity assays have been widely used as rapid, sensitive, and cost-effective analytical techniques in lab-on-paper devices (Wang et al., 2014a, 2014b; Apilux et al., 2012; Lutz et al., 2013). These devices have advantages such as high sensitivity, selectivity, rapid detection, and ability to analyze difficult matrices without extensive pretreatment. Enzyme-linked immunosorbent assay, the most extensively used type of immunoassay, was first developed for μ-PADs by Cheng et al. (2010). They also showed that a rapid immunoassay could be adapted to paper because of high surface-to-volume-ratio and faster immunoreaction. Thus, microfluidic paper-based immunodevices have been widely used to develop assays with a variety of detection strategies, including colorimetric and fluorescence-based detection (Oh et al., 2013).

Three-dimensional paper microfluidic devices use inexpensive methods to integrate complex fluid networks and detection zones, such as electrochemical cells. These characteristics allow for applications such as point-of-care diagnostics and environmental monitoring. However, many 3D devices involve time-consuming fabrication processes. These devices are fabricated layer-by-layer, which does not lend itself to mass production. The layers are typically held together with double-sided tape, and holes are cut into the device with sophisticated tools such as laser cutters. Three-dimensional folded paper microfluidic devices were developed by the Crooks group in 2011 with the goal of alleviating the complexities involved in fabrication of 3D devices (Thom et al., 2014) Folding precludes complicated alignment procedures and exact cutting. These initial devices utilized fluorescence and colorimetric detection, but ECL-based microfluidic devices and paper chips (Delaney et al., 2013) were soon reported.

6.1. Genosensors

Detecting very low concentrations of specific DNA sequences is required in clinical diagnostics, gene therapy, food safety, environment, and biodefense applications. The ECL nucleic-acid assay for μ-PADs promises a highly sensitive and reliable diagnosis. Nucleic acid assays are more suitable than antigen and/or antibody-based immunoassays for early detection of genetic and infectious diseases via μ-PADs (Veigas et al., 2012; Lo et al., 2013). The high precision of nucleic acid assays is due to base-pairing interactions between the complementary sequences. These interactions are more specific and vigorous than the interactions between antigens and antibodies. A nucleic acid assay using μ-PADs requires two types of oligonucleotide probes namely, detector probe (S_2) and capture probe (S_1). Both the detector and S_1 and S_2 are complementary to their target nucleic-acid sequence, and the detector probe is tag with a luminophore to make the reaction visible or measurable. The tag can be used for colorimetric assays (Song et al., 2014; Laopa et al., 2013; Yildiz et al., 2012; Veigas et al., 2012), electrochemical measurements (Lu et al., 2012) or fluorescent reporting (Allen et al., 2012) via μPADs. Functional nucleic acids, especially aptamers, are nucleic acids whose functions include nucleic-acid hybridization. To functionalize μ-PADs, aptamers are chosen as molecular probes because of their striking features such as superior affinity and specificity, ease of chemical modification, high stability, and low immunogenicity. Aptamer-based μ-PADs can be used to specifically detect a wide range of analytes from ions to proteins (Lewis et al., 2014; Yan et al., 2013). More importantly, the aptamer offers remarkable convenience and flexibility to design its structures, resulting in novel sensing strategies for μ-PADs with high sensitivity and selectivity. Furthermore, the small size and versatility of aptamers enable efficient immobilization at high density, which is vitally important in multiplexing miniaturized systems.

Using a single aptamer sequence, Li et al. (2014b) developed a simple, low cost, sensitive sandwich ECL-DNA sensor for μ-PADs using grapheme-modified porous gold-paper. This paper 3D origami device is fabricated from cellulose paper as shown in Fig. 2A, i-iv. The AuNP layer is grown on the surface of the cellulose fibers to increase the conductivity of the sensing platform; this was accomplished using the method of Yan et al. (2013). A sandwich DNA hybridization ECL model was constructed to assess the analytical practicality of this device. The

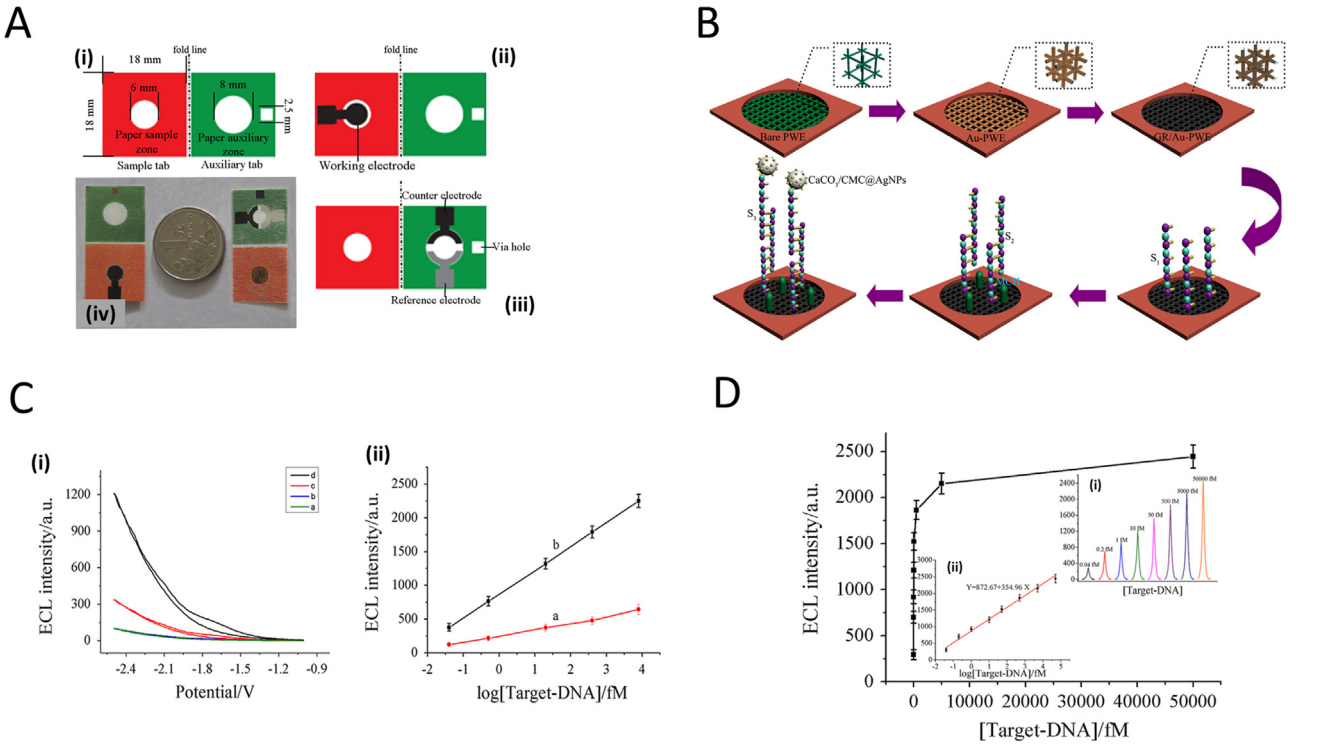

Fig. 2. Schematic representation of a μ-PAD (A). Representation of size and shape of a μ-PAD (A-i). One side of the μ-PAD contains the screen-printed working electrode (A-ii). The reverse side of (A-i) contains the screen-printed reference and counter electrodes (A-iii). Images of the entire μ-PAD (A-iv). Schematic representation of fabrication procedures for the μ-PAD DNA sensor (B). Curves of ECL potential obtained at different steps of electrode modification in 10 mM Tris–HCl buffer; pH 7.4 (C-i). ECL intensity profiles of the DNA sensor vs. concentration of S_2 obtained using: pure AgNPs (C-ii, Curve a) and CaCO3/CMC@AgNP-labeled S_3 (C-ii, Curve b). Relationship between ECL intensity and S_2 concentration at pH 7.4 (D). Inset (D-i) shows ECL intensity profiles of the DNA sensor in the presence of various concentrations of S_2; inset (D-ii) shows a logarithmic calibration curve of the ECL signals (Inset D-i) for S_2 (Li et al., 2014b).

Au-PWE is modified with positively charged PDDA-GR to immobilize the S_1. For hybridization, the DNA-modified electrode is allowed to react with target DNA (S_2) over the desired time. The DNA probe S_1, which is complementary to the probe S_2, undergoes hybridization to form the S_1-S_2 DNA hybrid structure. Subsequently, the electrode is hybridized with the reporter probe containing calcium carbonate/carboxymethyl chitosan (CaCO3/CMC) hybrid microspheres @ luminescent silver nanoparticles (AgNPs) (S_3–$CaCO_3$/CMC@AgNP bioconjugates) for 2 h at 37 °C. Hybridization (the S_2-S_3 binding hybrid) increases the concentration of $CaCO_3$/CMC@AgNP bioconjugates in the paper sample zone, resulting in increased ECL intensity in the presence of 0.1 M $K_2S_2O_8$ and 0.1 M KCL (Fig. 2B). The ECL emission is amplified in the presence of S_3–$CaCO_3$/CMC@AgNPs compared with that achieved in the presence of PDDA-GR/Au-PWE and S_2/S_1/PDDA-GR/Au-PWE (Fig. 2C, curve a). Quantitative behavior of the DNA sensor, assessed by monitoring ECL intensity at different concentrations of S_2 at optimal conditions; ECL emission intensity is directly related to the concentration of S_2 (Fig. 2D, inset i). ECL intensity increases linearly as S_2 concentration increases, showing the range of 4.0×10^{-17} to 5.0×10^{-11} M (Fig. 2D, inset ii). The limit of detection (LOD) was 8.5×10^{-18} M, showing acceptable quantitative behavior (Fig. 2D). The sensor shows higher dynamic range and detection limit in comparison to device reported by Feng et al. (2015); due to the fast electron transfer achieved by deposition of AuNP layer on sensing electrode platform and dual signal amplification effect of GR modified Au-PWE and CaCO3/CMC@AgNPs composites.

6.2. Cytosensors

Early and reliable cancer diagnosis provides an easier way to the effective and ultimately successful treatment of cancer. In terms of cancer diagnosis and therapy, sensitive and selective detection of cancer cells is vital and essential. Till date, numerous techniques, mostly based on fluorescence imaging, have been well developed to enumerate cancer cells (Farace et al., 2011; Bamrungsap et al., 2015; Pedram et al., 2015). Nevertheless, they are expensive, time-consuming, and require well-skilled technicians for operation. Compared with the conventional electrochemical and chemiluminescent methods, the chemiluminescent response in ECL is initiated and controlled by the application of a specific electrochemical potential, thus, providing additional selectivity (Forster et al., 2009). Consequently, ECL becomes an important and powerful analytical tool for paper-based cyto-devices.

Wu et al. (2016) developed a portable and disposable aptamer-based cytosensor on paper for the detection of cancer cells and in-situ screening of anticancer drugs. The fabrication of this paper based ECL cyto-device (PECLCD) is shown in Fig. 3A. A layer of Au@Pd NPs, grown on the surface of cellulose fibers in the paper sample zone of PWE, enhances the conductivity and enlarges the effective surface area of the PWE. The surface of Au@Pd PWE is immobilized with the corresponding MCF-7 cell-specific aptamer sequence. To capture the cells via specific binding between the immobilized aptamers and cells, a homogenous suspension of MCF-7 tumor cells is added into the corresponding aptamer/Au@Pd-PWE. PtNi alloy particles, formed by the dealloying of PtNiAl source, is loaded with carbon dots via EDC-NHS coupling to form a PtNi@C-dot composite, which served as ECL label. A solution of PtNi@C-dot-ConA bioconjugates is applied on each paper working cell zone to load C-dots onto the surface of captured cancer cells. PtNi@C-dot-ConA binds to the captured MCF-7 cells via specific recognition between Con-A and mannose on the surface of the cells. The PtNi@C-dot-ConA bioconjugates participate in the ECL reaction with the added $K_2S_2O_8$ in the Au@Pd-PWE to produce a quantitative ECL emission peak. After the incorporation of PtNi@C-dot-ConA nanoprobe into the MCF-7/BSA/aptamer/Au@Pd-PWE, PtNi@C-dot-ConA binds to the captured MCF-7 cells through specific recognition between Con-A

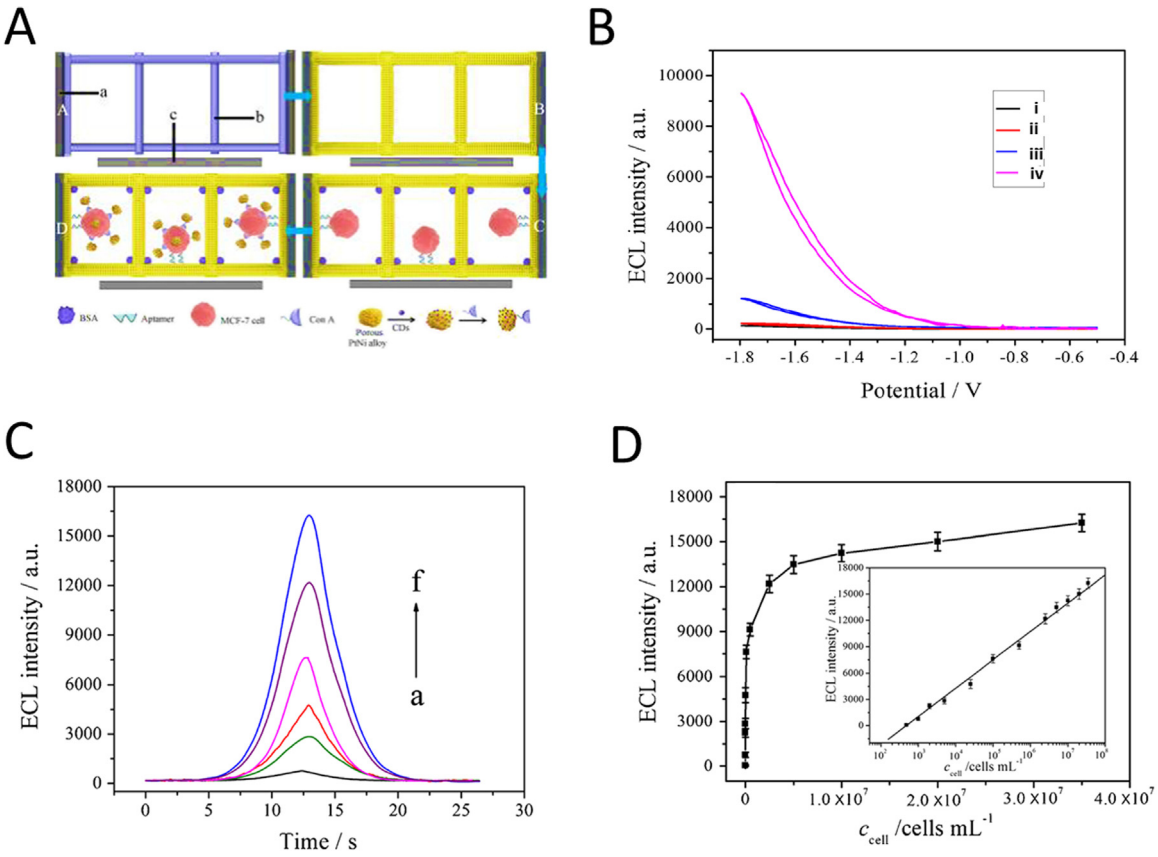

Fig. 3. Schematic representation of the fabrication procedure for paper-based ECL cytodevice (A). ECL-potential curves of the paper working electrode containing cell/BSA/aptamer/Au@Pd particles (curve b) with pure C-dots (curve c) and PtNi@C-dot labeled (curve d), and BSA/aptamer/Au@Pd-PWE in absence of cells (curve a) in PBS containing 0.1 M $S_2O_8^{2-}$. ECL responses of this paper-based cyto-device incubated with different concentrations of MCF-7 cells (from down to top: 10^3, 5×10^3, 2.5×10^4, 10^5, 2.5×10^6, and 3.5×10^7 cells. mL^{-1}, respectively) (C). Relationship between ECL response and cell concentration. Inset: Corresponding calibration curve for MCF-7 cell (D) (Wu et al., 2016).

and mannose on the surface of cells (Fig. 3B). The ECL curves for the PtNi@C-dot was measured in 0.01 M PBS buffer (pH 7.4) containing 0.1 M $K_2S_2O_8$ and 0.1 M KCl. The ECL intensity of cyto-sensor using PtNi@C-dot labeled cells (Fig. 3B, curve iv) is about 8-fold greater than that of the pure C-dots (Fig. 3B, curve iii), which may be due to high capacity of loading C-dots as well as good electric conductivity and biocompatibility of the PtNi@C-dot composites. In this case, the ECL response is based on the electron-transfer between the reduced species formed in PtNi@C-dot and oxidized species of the co-reactant ($S_2O8_2^-$). The ECL intensity of this cyto-sensor for the sensitive detection of cancer cells increases logarithmically over a wide concentration range of $4.8 \times 10^2 - 2.0 \times 10^7$ cells mL^{-1}, and with a detection limit of 300 cells mL^{-1} (Fig. 3C & D). The device shows a greater dynamic range than Feng et al. (2014a) and Yang et al. (2017), but a lower detection limit than Feng et al. (2014a), Wu et al. (2015a), and Yang et al. (2017).

Yang et al. (2017) developed a Sudoku-like cytodevice with dual enhancement of ECL intermediates. This 3D origami device is fabricated from inexpensive cellulose paper as shown in Fig. 4A. Once after device fabrication, semicarbazide and AuNPs are alternatively deposited onto the surface of AuNR-modified PWE, forming $(AuNPs-SE)_2-AuNR-PWE$. The aptamers, specific for cancer cells, are immobilized on the corresponding working zones of the test tab. A mixture, containing Ag−MBdsDNA and a homogeneous cell suspension at a specified concentration, is applied on the corresponding aptamers/$(AuNPs-SE)_2-AuNRs-PWE$. Tumor cells and Ag−MBdsDNA are captured on the corresponding cytozone via specific recognition of aptamers by target cells and hybridization of aptamers with exposed DNA initiators of Ag−MBdsDNA. The Ag−MBdsDNA and target cells competitively interact with the aptamers fixed on the electrode; thereby, Ag−MBdsDNAs are trapped on the sensing interface. Subsequently, GQDs are assembled on the three-dimensional (3D) DNA skeleton of the captured Ag−MBdsDNA via π−π stacking. Because of their good self-catalytic activity, the labeled AgNPs induce catalytic silver deposition on Ag−MBdsDNA@GQDs, achieving maximal signal amplification (Fig. 4B). The simultaneous and ultrasensitive detection of four types of cancer cells is achieved by converting the cell content into the final loading quantity of light-switching Ag−MBdsDNA@GQDs. Four types of cancer cells, MCF-7, CCRF-CEM, HeLa, and K562, were assayed in the ranges of 1.0×10^2–1.0×10^7, 1.5×10^2–2.0×10^7, 2.0×10^2–5.0×10^6, and 1.2×10^2–2.0×10^6 cells mL^{-1}, with the detection limits of 38, 53, 67, and 42 cells mL^{-1}, respectively (Fig. 4C & D). The cytodevices are very specific, and different types of tumor cells could be detected simultaneously by modifying the working electrode with different sensing aptamers. These devices have potential applications for early tumor detection.

6.3. Tumor markers immunosensors

Increased levels of tumor markers, including proteins, enzymes and peptide hormones, in human serum are significantly associated with certain tumor or carcinoma. Thus, rapid, quantitative and sensitive detection of tumor markers in human serum is essential for early diagnosis and treatment (Daar et al., 2002). Immunoassay is a common bio-analytical method that measures tumor markers using the reaction of an antibody to its antigen (Yeh et al., 2009). Until now, immunoassays, including radioimmunoassays (Zhang et al., 2010), enzyme-linked immunosorbent assay (ELISA) (Lai et al., 2004),

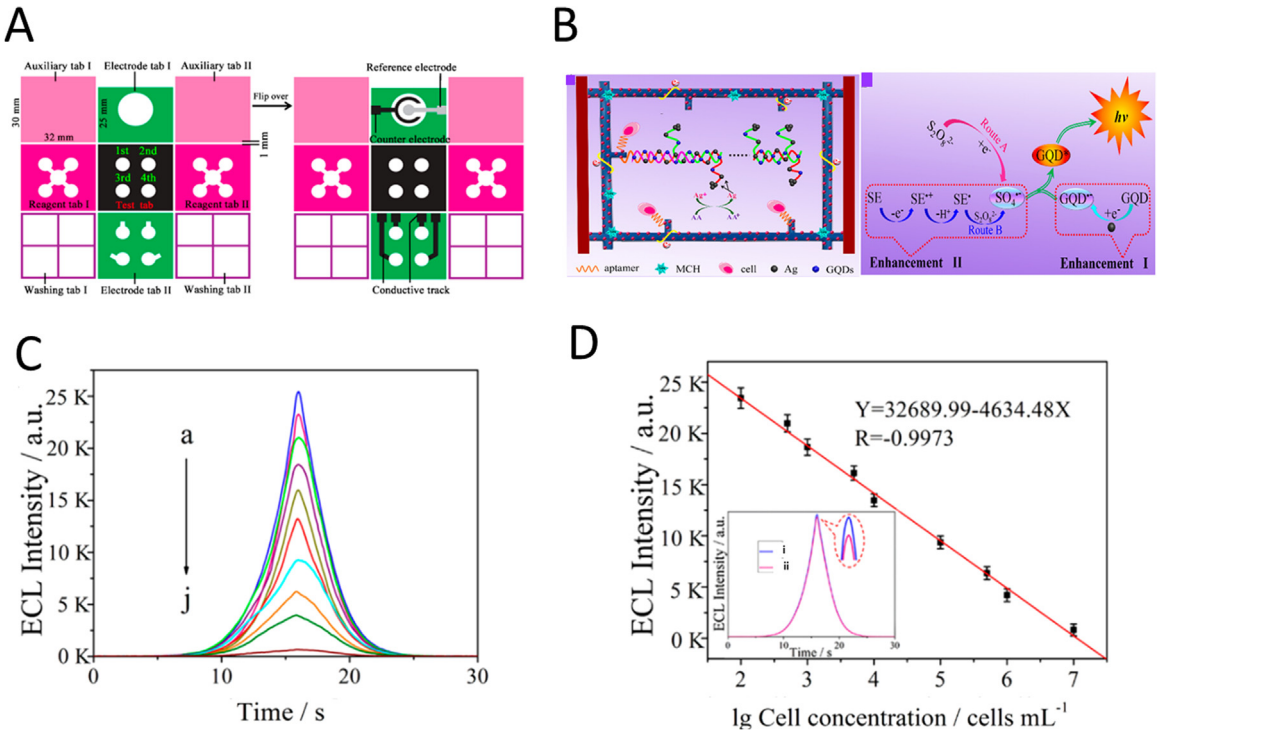

Fig. 4. Schematic Layout for Size, and Shape of the Integrated Lab-on-Paper Device (A). Schematic Representation of the Fabrication procedures and ECL analytical principle of sudoku-like origami-based ECL cyto-device (B). ECL profiles of the sudoku-like origami-based ECL cyto-device incubated with different concentrations of MCF-7 cells (C). The corresponding calibration curve with an inset: the ECL response of the cyto-sensor, without (i) and with (ii) MCF-7 incubation, 38 cells mL^{-1} (D) (Yang et al., 2017).

chemiluminescence immunoassay (CLIA) (Bi et al., 2009) and piezoelectric immunosensors (Zhou et al., 2013) have been widely reported for tumor markers detection. However, most of the above-mentioned methods usually remain cumbersome, time-consuming, and harmful to the operator health. Therefore, it is of considerable interest to the further research for sensitive, accurate, rapid and simple alternative methodology for determination of tumor markers. Compared with the conventional electrochemical immunoassays, the ECL immunoassay combined with paper microfluids has become one of the predominant analytical techniques for its intrinsic advantages such as fast response time, simple instrumentation, wide dynamic concentration response range and excellent detection sensitivity for electrochemical and a very high specificity for immunoassays during the recent years.

Wang et al. (2013) developed a 3D microfluidic origami ECL immunodevice for sensitive point-of-care testing of carcinoma antigen 125 in clinical serum samples. The fabrication of this microfluidic origami device on pure cellulose paper is presented under Fig. S1, A. To increase the rate of electron transfer and enhance the immobilization of capture antibody (Ab_1), the working electrode zone is immobilized with AuNPs. The luminol-AuNPs are used as ECL luminophores and are conjugated to the signal antibodies of the ECL sandwich immunoreaction (Fig. 5A). The sandwich immunosensor shows an intense ECL emission peak upon addition of CA125 (Fig. S1, B). The sensor shows a linear increase in ECL intensity with increasing concentration of CA125 over the range of 0.01–100 U mL^{-1} and a detection limit of 0.0074 U mL^{-1} (Fig. 5B). The sensor linear range is higher than the studies reported by Ge et al. (2012), Liu et al. (2014), Li et al. (2014c) and lower than the studies reported by Zhang et al. (2013c), Li et al. (2013c). On the other hand, the detection limit is lower than the studies reported by., 2012; Liu et al. (2014), Li et al. (2014c), Zhang et al. (2013c), Li et al. (2013c). All these devices have potential applications for making point of care clinical assays in remote regions and developing countries.

A similar immune device was developed to detect the tumor marker CEA (Yan et al., 2014). In this device, the working electrode is functionalized with graphene and gold. The phenyleneethynylene derivative modified nanotubular mesoporous Pt–Ag alloy nanoparticles (Pt-Ag ANPs) were synthesized by following the method reported by Yan et al. (2012b) and used as signal amplifier for sensitive detection of the analyte. CEA was detected in human serum over a linear range of 0.001 ng mL^{-1} to 100 ng mL^{-1} with a detection limit of 0.3 pg mL^{-1}. The device shows a higher dynamic range and detection limits than the reports studied by Li et al. (2014a); Ge ta l., 2012; Sun et al. (2018), and a lower dynamic range and detection limit in comparison to Li et al. (2013a); Gao et al., 2015; and Li et al. (2013b). This group also developed an ECL sandwich immunoassay for the sensitive detection of CEA in serum using a 3D origami paper device (Gao et al., 2015). This device uses a paper working electrode modified with Ag nanospheres (Ag-PWE) as a sensor platform and Au nanocages functionalized with tris-(bipyridine)-ruthenium(II) $[Ru(bpy)_3]^{2+}$ as ECL signal-amplification label. A novel Ag-PWE, having high conductivity, is fabricated by growing a layer of Ag nanospheres on the surface of cellulose fibers to provide rapid electron transfer and enhance the amount of Ab_1. CEA is detected in human serum samples with a linear range of 0.001–50 ng mL^{-1} and a detection limit of 0.0007 ng mL^{-1}. Sun et al. (2018) developed a rotational paper-based analytical ECL device for multiplexed detection of cancer biomarkers. The fabrication of this rotational paper-based immunodevice is presented under Fig. S2, A & B. This device was fabricated using the method by Li et al. (2017b). The immunozones on the detection disc are modified with MWCNT and chitosan composites. The Ab_1's, specific for CEA and PSA, are immobilized via glutaraldehyde cross-linking. Adding the antigens CEA and PSA to the corresponding immunozones and incubating with the $[Ru(bpy)_3]^{2+}$-labeled signaling antibodies establishes sandwich ECL immunocomplexes on the rotational device (Fig. 6A). This rotational device showed a good analytical performance for CEA and PSA over the linear ranges of 0.1–100 ng mL^{-1} and 0.1–50 ng mL^{-1}, with detection limits of 0.07 ng mL^{-1} and 0.03 ng mL^{-1}, respectively (Fig. 6B). The dual analyte sensing device shows a very low dynamic range and detection

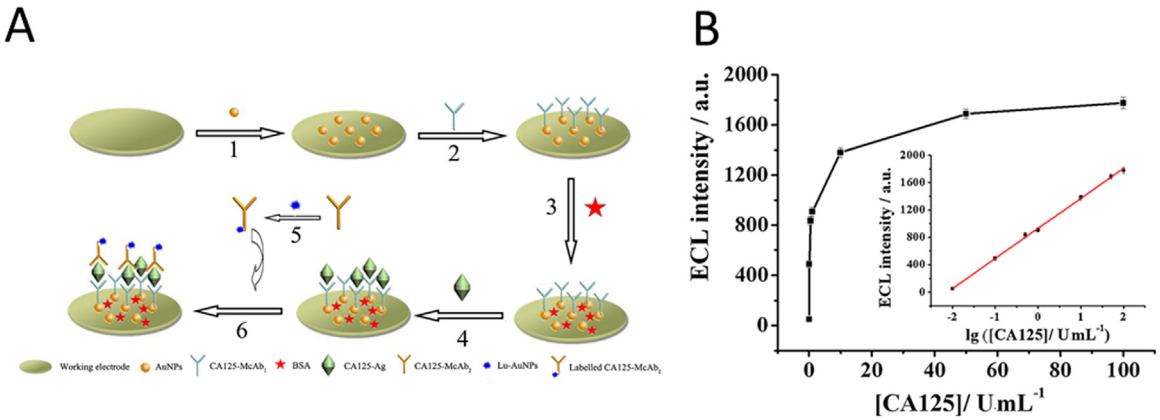

Fig. 5. Schematic representation of the ECL sandwich immunoassay procedure on the cellulose PWE (A). Relationship between ECL response and CA concentration, Inset: Corresponding linear calibration curve for CA (B) (Wang et al., 2013).

limits in compared to the other reports studied by Li et al. (2013b), Feng et al. (2014b). For convenience of the readers the comparison of the main analytical characteristics and the type of luminophores and sensor materials used in each case study for the paper-based ECL devices is shown in Table 1.

6.4. Metal ions sensors

Zhang et al. (2013a) developed a 3D microfluidic analytical device on cellulose paper for simultaneous ECL detection of two metal ions in a single paper electrode via covalent immobilization of the corresponding oligonucleotide (aptamer). The 3D paper-based ECL device was fabricated from a patterned pure cellulose paper as shown in Fig. 7A. After fabrication of the device, the aptamers are tagged with a terminal ECL label and covalently immobilized on the paper working zone of SPCWE. The silica nanoparticles capped with carbon nanocrystals (CNCs) (Si@CNCs) and $Ru(bpy)_3^{2+}$–gold nanoparticle (AuNP) aggregates (Ru@AuNPs) are both used as terminal ECL labels for Pb^{2+} and Hg^{2+} detection, respectively. The long, flexible, modified aptamer chain prevents electrical contact between the ECL label and the electrode in the absence of metal ions. Upon binding of aptamers to their target metal ions Pb^{2+} and Hg^{2+}, the immobilized aptamers fold their flexible, single-stranded chains into G-quadruplex and T–Hg–T complexes, respectively (Fig. 7B). The change in confirmation of the aptamer enables the electrical communication of the ECL label with the electrode, producing a positive ECL signal. The ECL intensity of the sensor for simultaneous detection of two metal ions increased with the increasing concentration of the analytes (Fig. 7C). The calibration plots show a good linear relationship between ECL intensity and analyte concentration in the range of 3.0×10^{-11} to 1.0×10^{-6} M for Pb^{2+} and 5.0×10^{-10} to 1.0×10^{-6} M for Hg^{2+} (Fig. 7D). The sensor also showed a good detection limit of 10 pM and 0.2 nM for Pb^{2+} and Hg^{2+}, respectively. Compared with those of single-analyte assays, the 3D paper-based ECL device showed a relatively larger linear range and lower detection limits (Han et al., 2009; Xiao et al., 2007; Xu et al., 2018). The assay was successfully applied to lake water and human serum samples and represents a simple, portable and economical method for environmental monitoring and clinical measurements. The main advantages of the method include (a) Detection of two different metal ions coexisting in one paper working zone, which simplifies the 3D paper-based device for low-cost POC analysis, (b) the potential control technique based on Si@CNCs and Ru@AuNPs, extended the application of ECL field

6.5. Glucose sensor

Chen et al. (2016) developed a handheld bipolar electrode ECL system on paper. Glucose is detected by immobilizing the GOD (1 U/μL) on the BPE anode via physical adsorption. To test this device, a luminol/H_2 O_2-based ECL reaction was first carried out to demonstrate the quantitative ability of the P-BPE-ECL system. The response to H_2O_2 was linear over the concentration range of 5.0–5000 μM. This device had a detection limit of 1.75 μM. The practical applicability of this P-BPE-ECL system was demonstrated by detecting glucose in a PBS and in artificial urine samples. The detection limits were 0.017 mM and 0.030 mM, respectively, over a concentration range of 0–5.0 mM, which are lower than the study reported by Doeven et al. (2015).

7. Summary and conclusion

A comprehensive review of the literature suggests that ECL-based devices can strongly compete with other more regularly used

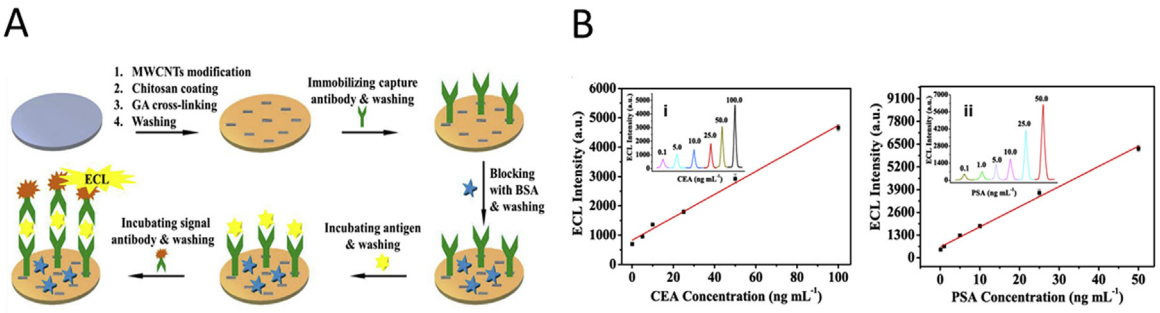

Fig. 6. Schematic representation of the ECL sandwich immunoassay procedure on the rotational paper disc device (A). Relationship between ECL intensity vs. CEA and PSA concentration at pH 7.4 (B); Inset (B-i & ii) shows ECL intensity profiles of the tumor marker sensor in the presence of various concentrations of CEA and PSA (Sun et al., 2018).

Table 1
Summary of the ECL paper based analytical devices by type of biomarker, ECL label, electrode material and figures of the merit.

Sensor material	Analyte	ECL luminophores	Electrode material	Dynamic range and detection limit	Reference
Metal ions	Pb^{2+}	Si@CNCs	NaIO4 Paper	3.0×10^{-11}–1.0×10^{-16} M	Zhang et al. (2013a)
Paper	Hg^{2+}	Ru@AuNPs		10 pM 5.0×10^{-10}–1.0×10^{-6} M 0.2 nM	
Paper	Pb^{2+}	rGO–PdAu–GOx	Au paper	0.5–2000 nM 0.14 nM	Xu et al. (2018)
Genosensors	ATP	P–acid-Pt-Ag-ANP	Au-Paper	0.5 pM–70 nM	Yan et al. (2013)
Origami Paper				0.1 pM	
Paper	DNA	$CaCO_3$/CMC@AgNP	Porous Au	4.0×10^{-17}–5.0×10^{-11} M 8.5×10^{-18} M	Li et al. (2014b)
Paper	Syphilis DNA	PtNPs	Carbon Bipolar	0.1–100 fmol L^{-1} 0.1 fmol L^{-1}	Feng et al. (2015)
	HIV DNA HBV DNA			0.5–100 fmol L^{-1} 0.5 fmol L^{-1} 0.2–100 fmol L^{-1} 0.2 fmol L^{-1}	
Paper	Pathogenic DNA	$[Ru(phen)_2dppz]^2$	Carbon Bipolar	$10–11 \times 10^6$ copies μL^{-1} 10 copies μL^{-1}	Liu et al. (2016)
Cytosensors	Cancer cells	Pt@Ni Carbon dots	Au@PdNP	4.8×10^2–2×10^7 cells mL^{-1} 3000 cells mL^{-1}	Wu et al. (2016)
Paper					
Paper	Cancer cells	AgNPs GQDs	$(AuNPs\text{-}SE)_2$-AuNRs	1.0×10^2–1.0×10^7 cells mL^{-1} 38 cells mL^{-1} 1.5×10^2–2.0×10^7 cells mL^{-1} 53 cells mL^{-1} 2.0×10^2–5.0×10^6 cells mL^{-1} 67 cells mL^{-1} 1.0×10^2–2.0×10^6 cells mL^{-1} 42 cells mL^{-1}	Yang et al. (2017)
Paper	Cancer cells	$RuSi@Ru(bpy)_3^{2+}$ -NP	AuNPs-GA-CS	0–5.6×10^6 cells mL^{-1} 56 cells mL^{-1}	Feng et al. (2014a)
Paper	Cancer cells	Au-PdNPs	AuNPs	$450–10 \times 10^7$ cells mL^{-1} 250 cells mL^{-1}	Wu et al. (2015a)
Tumor biomarkers	CA125	Luminol-AuNPs	AuNPs	0.01–100 U mL^{-1} 0.0074 U mL^{-1}	Wang et al. (2013)
Paper					
Paper	CEA	P-acid/Pt-AgNPs	GO-AuNPs	0.001–100 ng mL^{-1} 0.3 pg mL^{-1}	Yan et al. (2014)
Paper	CEA	CdTe@AgNPs	Porous AgNPs	0.5–20 pg mL^{-1} 0.12 pg mL^{-1}	Li et al. (2013a)
Origami Paper	CEA	$[Ru(bpy)_3]^{2+}$AgNanospheres	Aunanocages	0.001–50 ng mL^{-1} 0.0007 ng mL^{-1}	Gao et al. (2015)
Origami Paper	CEA	GQDs/Au@PtNps	NPG	1.0 ng mL^{-1} – 10 ng mL^{-1} 0.6 pg mL^{-1}	Li et al. (2014a)
Paper	AFP CA125 CA199 CEA	$[Ru(bpy)_3]^{2+}$	Chitosan	0.5–100 ng mL^{-1} 0.15 ng mL^{-1} 1.0–100 U mL^{-1} 0.6 U mL^{-1} 0.5–100 U mL^{-1} 0.17 U mL^{-1} 1.0–100 ng mL^{-1} 0.5 ng mL^{-1}	Ge et al. (2012)
Paper	PSA CEA	P-acid–/NPS	GO-CS/Au	0.003–20 ng mL^{-1} 1.0 pg mL^{-1} 0.001–10 ng mL^{-1} 0.8 pg mL^{-1}	Li et al. (2013b)
Paper	AFP	N-GQDs	Au nanoflowers	0.005–100 ng mL^{-1} 1.2 pg mL^{-1}	Zhang et al. (2015)
Paper	CA125	NH_2-MSNs	AgNPs	0.01–50 U mL^{-1} 4.3 mU mL^{-1}	Liu et al. (2014)
Paper	CA125	CdTeQDs@CMs	GN–Ag–Au	0.008–50 U mL^{-1} 2.5 mU mL^{-1}	Zhang et al. (2013c)
Paper	CA125	Pd@AuNPs/GOx	Ag@Au hybrids	0.1–100 U mL^{-1} 0.06 mU mL^{-1}	Li et al. (2014c)
Paper	CEA CA125 AFP	$[Ru(bpy)_3]^{2+}$ Luminol CdTe QDs	Nanoporous Ag Nanoporous Ag Nanoporous Ag	10 pg mL^{-1} – 50 ng mL^{-1} 0.8 pg mL^{-1} 5 mU mL^{-1}–50 U mL^{-1} 1.2 mU mL^{-1} 3.0 pg mL^{-1}–50 ng mL^{-1} 1.0 pg mL^{-1}	Li et al. (2013c)

(*continued on next page*)

Table 1 (*continued*)

Sensor material	Analyte	ECL luminophores	Electrode material	Dynamic range and detection limit	Reference
Paper	AFP CEA CA153 CA199	$[Ru(bpy)_3]^{2+}$ And CNDs	MWCNTs/CS	N.R 0.02 ng mL^{-1} N.R 60 mU mL^{-1} N.R 50 mU mL^{-1} N.R 4.0 pg mL^{-1}	Wang et al. (2012b)
Paper	PSA	SiO_2/GOx	MWCNTs	1.0 pg mL^{-1} -100 ng mL^{-1} 1.0 pg mL^{-1}	Feng et al. (2014b)
Paper	CA199	Ru@AuNPs	chitosan	0.01–200 U mL^{-1} 0.0055 U mL^{-1}	Yang et al. (2014)
Paper	CEA PSA	$[Ru(bpy)_3]^{2+}$	MWCNTs/CS	0.1–100 ng mL^{-1} 0.07 ng mL^{-1} 0.1–50 ng mL^{-1} 0.03 ng mL^{-1}	Sun et al. (2018)
Glucose Paper	Glucose	Luminol	Carbon Bipolar	5.0–5000 μM 1.75 μM	Chen et al. (2016)
Paper	Glucose	Luminol	Carbon self -powered	10 nM–10 mM 1.7 nM	Doeven et al. (2015)
Miscellaneous Paper	Amyloid β-protein	$[Ru(phen)_2dppz]^2$	Carbon paper	N.R 100 pM	Liu et al. (2018)
Paper	DBAE	$[Ru(bpy)_3]^{2+}$	Carbon paper	0–10 Mm 5 mM	Delaney et al. (2013)
OrigamiPaper	HCG	$[Ru(bpy)_3]^{2+}$	NPG	0.005–4000 U mL^{-1} 0.0019 U mL^{-1}	Wang et al. (2012a)
Origami paper	H_2S	Graphene quantum dots	Au@PtNP	N.R 10-7 M	Li et al. (2015)

N.R: not reported.

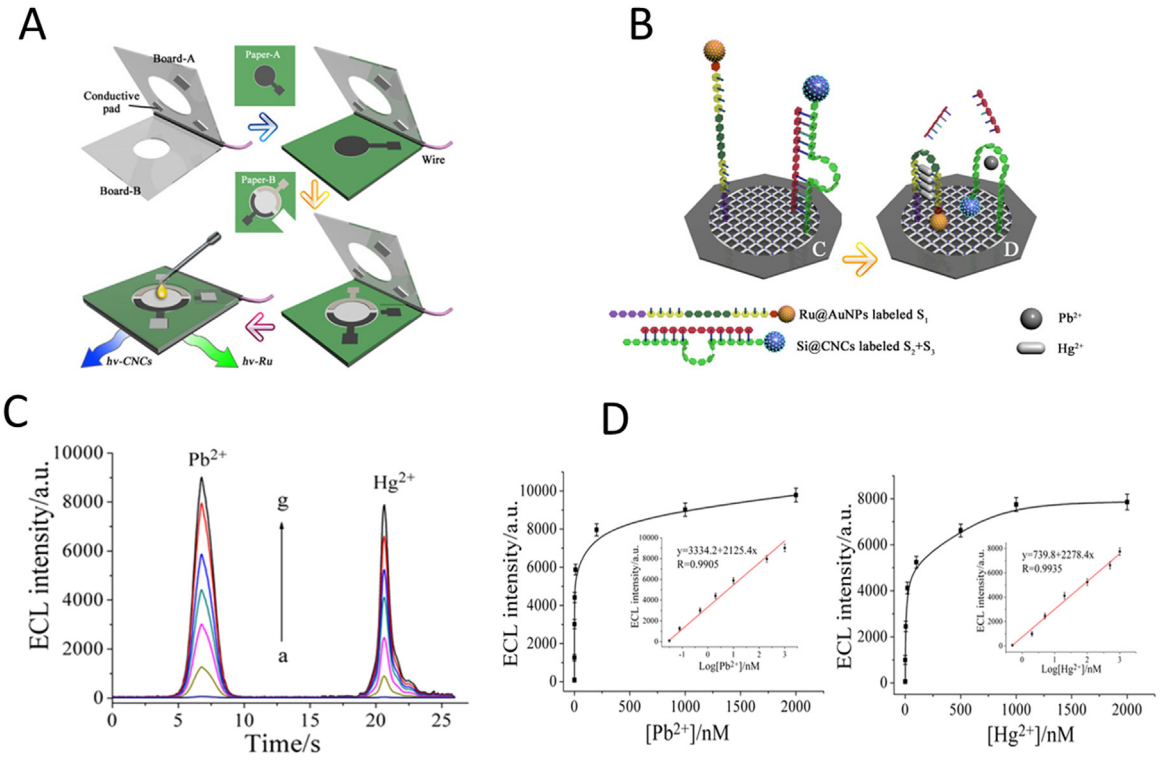

Fig. 7. Schematic representation of a 3D paper-based ECL device (A). SPCWE showing immobilized Ru@AuNP-labeled DNA strands for Hg^{2+} (Right) and Si@CNC-labeled DNA strands for Pb^{2+} (Left); change in confirmation of the aptamers after capturing with Pb^{2+} and Hg^{2+} (B). ECL intensity profiles with the increasing concentration of Pb^{2+} and Hg^{2+}, in 10 mm Tris–HCl buffer (pH 7.4) (C). Calibration curves of a 3D paper-based ECL sensor for determination of Pb^{2+} and Hg^{2+} concentration. The inset shows ECL peak intensity vs. concentration of Pb^{2+} and Hg^{2+} plotted on a logarithmic scale (D) (Zhang et al., 2013a).

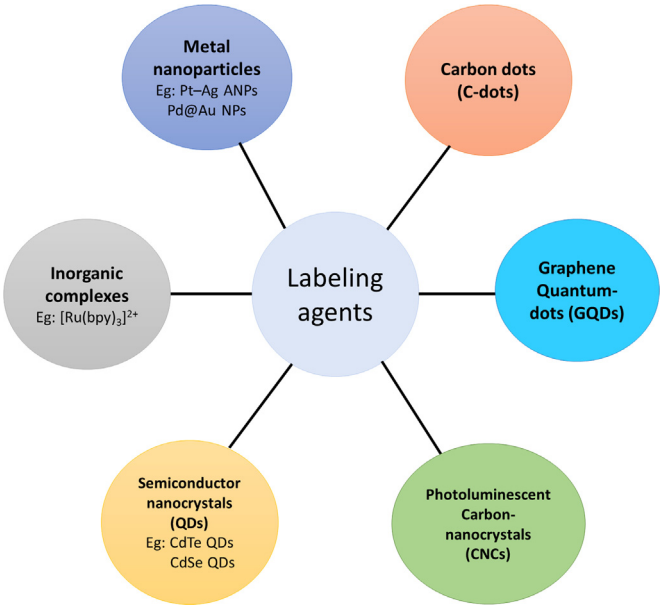

Scheme 1. Schematic representation of the various labeling agents used in ECL paper-based sensors.

transduction principles based on electrochemistry. The distinguishing features of ECL techniques and demands in various fields have led to the development of new assays and applications in clinical diagnostics, biodefense, food and water safety, and environmental analysis. Miniaturized systems, using immobilized reagents on cellulose paper and nanoscale technology, have enhanced the analytical performance of these ECL biosensors. The advantages of ECL paper-based biosensors in comparison to the other transduction principle based on electrochemistry, fluorescence and chemiluminescence include ultrasensitive detection and portable point-of-care testing using affinity-based recognition elements ranging from antibodies, molecularly imprinted polymers, aptamers and nucleic acids. Miniaturization of ECL instruments spurs the development of portable devices for point-of-care testing. These ongoing demands will open new and promising strategies in the design of ECL immunosensors, encouraging researchers to: (a) design diverse types of nanomaterials as new electrode materials for functional sensor modification (immobilization support) aimed at ECL signal amplification, and as new types of efficient labels; (b) to construct integrated systems for applications in POC diagnostics. In conclusion, ECL microfluidic paper-based analytical devices will continue to be a thriving area of research in the coming years.

8. Future perspectives

Despite advances in paper-based ECL biosensors, experimental models have not yet been translated into the industrial production of these instruments or wide application of these devices in practice. New low-toxicity, environmentally friendly materials are still needed to improve the sensitivity and long-term stability of ECL paper-based devices. More research is required to identify and design new co-reactants that will be superior to TPrA and DBAE. Although $Ru(bpy)_3^{2+}$ is a well-characterized and highly versatile ECL emitter, we need reagents that are equally stable but possess a higher ECL efficiency. Reagents that emit at different wavelengths are also highly sought after. Furthermore, we need to develop ultra-sensitive assays by employing amplification techniques. Understanding the key aspects of the design of ECL paper devices, testing parameters (LOD, specificity, assay speed, detection format, sample matrices, packaging, labeling, stability requirements, and target cost), and manufacturing processes will help provide a framework for further development of ECL paper analytical devices. The new generations of these devices may have the advantages of enhanced detection throughput and lowered detection cost (Scheme 1).

Acknowledgements

The work was supported by the National Research Foundation of Korea, Republic of Korea. (Grant No. NRF 2017R1D1A1A09000712, 2018R1C1B6009385, 2018M3A9F1023690).

Appendix A. Supporting information

Supplementary data associated with this article can be found in the online version at doi:10.1016/j.bios.2018.10.038

References

Akyazi, U., Desmonts, L., Benito-Lopez, F., 2018. Anal. Chim. Acta 1001, 1–17.
Allen, P.B., Arshad, S.A., Li, B., Chen, X., Ellington, A.D., 2012. Lab Chip 12, 2951–2958.
Amelia, M., Lincheneau, C., Silvi, S., Credi, A., 2012. Chem. Soc. Rev. 41, 5728–5743.
Apilux, A., Dungchai, W., Siangproh, W., Praphairaksit, N., Henry, C.S., Chaila-pakul, O., 2010. Anal. Chem. 82, 1727–1732.
Apilux, A., Ukita, Y., Chikae, M., Chilapakul, O., Takamura, Y., 2012. Lab Chip 13, 126–135.
Baker, S.N., Baker, G.A., 2010. Angew. Chem. Int. Ed. 49, 6726–6744.
Bamrungsap, S., Treetong, A., Apiwat, C., Wuttikhun, T., Dharakul, T., 2015. Microchim. Acta 183, 249–256.
Bard, A.J., 2004. Electrogenerated Chemiluminescense. Marcel Dekker, New York.
Bertoncello, P., Forster, R.J., 2009. Biosens. Bioelectron. 24, 3191–3200.
Bertoncello, P., Stewart, A.J., Dennany, L., 2014. Anal. Bioanal. Chem. 406, 5573–5587.
Bertoncello, P., Ugo, P., 2017. ChemElectroChem 4, 1663–1676.
Bi, S., Zhou, H., Zhang, S., 2009. Biosens. Bioelectron. 24, 2961–2966.
Bruchez, M., Moronne, M., Gin, P., Weiss, S., Alivisatos, A.P., 1998. Science 281, 2013–2016.
Chan, W.C.W., Nie, S., 1998. Science 281, 2016–2018.
Chen, L., Zhang, C., Xing, D., 2016. Sens. Actuators B: Chem. 237, 308–317.
Cheng, C.-M., Martinez, A.W., Gong, J., Mace, C.R., Phillips, S.T., Carrilho, E., Mirica, K.A., Whitesides, G.M., 2010. Angew. Chem. Int. Ed. 49, 4771–4774.
Chin, C.D., Laksanasopin, T., Cheung, Y.K., Steinmiller, D., Linder, V., Parsa, H., Wang, J., Moore, H., Rouse, R., Umviligihozo, G., Karita, E., Mwambarangwe, L., Braunstein, S.L., Van De Wijgert, J., Sahabo, R., Justman, J.E., El-Sadr, W., Sia, S.K., 2011. Nat. Med. 17, 1015–1019.
Cummins, B.M., Ligler, F.S., Walker, G.M., 2016. Biotechnol. Adv. 34, 161–176.
Daar, A.S., Thorsteinsdóttir, H., Martin, D.K., Smith, A.C., Nast, S., Singer, P.A., 2002. Nat. Genet. 32, 229–232.
de Araujo, W.R., Paixao, T.R.L.C., 2014. Analyst 139, 2742–2747.
Delaney, J.L., Hogan, C.F., Tian, J., Shen, W., 2011. Anal. Chem. 83, 1300–1306.
Delaney, J.L., Doeven, E.H., Harsant, A.J., Hogan, C.F., 2013. Anal. Chim. Acta. 803, 123–127.
Deng, S., Ju, H., 2013. Analyst 138, 43–61.
Deng, Z.T., Schulz, O., Lin, S., Ding, B.Q., Liu, X.W., Wei, X.X., Ros, R., Yan, H., Liu, Y., 2010. J. Am. Chem. Soc. 132, 5592–5593.
Derfus, A.M., Chan, W.C.W., Bhatia, S.N., 2004. Nano Lett. 4, 11–18.
Doeven, E.H., Barbante, G.J., Harsant, A.J., Donnelly, P.S., Connell, T.U., Hogan, C.F., Francis, P.S., 2015. Sens Actuators B: Chem. 216, 608–613.
Du, F.K., Zeng, F., Ming, Y.H., Wu, S., 2013. Microchim Acta 180, 453–460.
Esteve-Turrillas, F.A., Abad-Fuentes, A., 2013. Biosens. Bioelectron. 41, 12–29.
Farace, F., Massard, C., Vimond, N., Drusch, F., Jacques, N., Billiot, F., Laplanche, A., Chauchereau, A., Lacroix, L., Planchard, D., Le Moulec, S., Andre, F., Fizazi, K., Soria, J.C., Vielh, P., 2011. Br. J. Cancer 105, 847–853.
Feng, Q., Liu, Z., Chen, H., Xu, J.-J., 2014a. Electrochem. Commun. 49, 88–92.
Feng, Q., Chen, H., Xu, J., 2015. J. Sci. China Chem. 58, 810–818.
Feng, Q., Pan, J., Zhang, H., Xu, J., Chen, H., 2014b. Chem. Commun. 50, 10949–10951.
Forster, R.J., Bertoncello, P., Keyes, T.E., 2009. Annu. Rev. Anal. Chem. 2, 359–385.
Gao, C., Su, M., Wang, Y., Ge, S., Yu, J., 2015. RSC Adv. 5, 28324–28331.
Ge, L., Yan, J., Song, X., Yan, M., Ge, S., Yu, J., 2012. Biomaterials 33, 1024–1031.
Ge, L., Yu, J., Ge, S., Yan, M., 2014a. Anal. Bioanal. Chem. 406, 5613–5630.
Ge, S., Liu, F., Liu, W., Yan, M., Song, X., Yu, J., 2014b. Chem. Commun. 50, 475–477.
Glavan, A.C., Martinez, R.V., Subramaniam, A.B., Yoon, H.J., Nunes, R.M.D., Lange, H., Thuo, M.M., Whitesides, G.M., 2013. Adv. Funct. Mater. 24, 60–70.
Gross, E.M., Durant, H.E., Hipp, K.N., Lai, R.Y., 2017. ChemElectroChem 4, 1594–1603.
Gu, W., Xu, Y., Lou, B., Lyu, Z., Wang, E., 2014. Electrochem. Commun. 38, 57–60.
Haller, P.D., Flowers, C.A., Gupta, M., 2011. Soft Matter 7, 2428–2432.
Han, D.H., Kim, Y.R., Oh, J.W., Kim, T.H., Mahajan, R.K., Kim, J.S., Kim, H., 2009. Analyst 134, 1857–1862.
Han, Y.L., Wang, W., Hu, J., Huang, G., Wang, S., Lee, W.G., Lu, T., Xu, F., 2013. Lab Chip 13, 4745–4749.
Huang, X.Q., Li, X.J., Chen, Y., Zhou, E.B., Xu, Y.X., Zhou, H.L., Duan, X.F., Huang, Y., 2013. Angew. Chem. Int. Ed. 52, 2520–2524.
Jia, F., Lv, S., Xu, S., 2017. RSC Adv. 7, 53532–53536.
Kakoti, A., Siddiqui, M.F., Goswami, P., 2015. Biomicrofluidics 9, 026502.
Klasner, S.A., Price, A.K., Hoeman, K.W., Wilson, R.S., Bell, K.J., Culbertson, C.T., 2010.

Anal. Bioanal. Chem. 397, 1821–1829.
LaGasse, M.K., Rankin, J.M., Askim, J.R., Suslick, K.S., 2014. Sens. Actuators B: Chem. 197, 116–122.
Lai, S., Wang, S.N., Luo, J., Lee, L.J., Yang, S.T., Madou, M.J., 2004. Anal. Chem. 76, 1832–1837.
Laopa, P.S., Vilaivan, T., Hoven, V.P., 2013. Analyst 138, 269–277.
Lewis, G.G., Robbins, J.S., Phillips, S.T., 2014. Chem. Commun. 50, 5352–5354.
Li, B., Yu, L., Qi, J., Fu, L., Zhang, P., Chen, L., 2017a. Anal. Chem. 89, 5707–5712.
Li, L., Chen, Y., Zhu, J.-J., 2017b. Anal. Chem. 89, 358–371.
Li, L., Li, W., Ma, C., Yang, H., Ge, S., Yu, J., 2014a. Sens Actuators B: Chem. 202, 314–322.
Li, M., Wang, Y., Zhang, Y., Yu, J., Ge, S., Yan, M., 2014b. Biosens. Bioelectron. 59, 307–313.
Li, W., Li, L., Li, S., Wang, X., Li, M., Wang, S., Yu, J., 2013a. Sens Actuators B: Chem. 188, 417–424.
Li, W., Li, M., Ge, S., Yan, M., Huang, J., Yu, J., 2013b. Anal. Chim. Acta 767, 66–74.
Li, W., Yang, H., Ma, C., Li, L., Ge, S., Song, X., Yu, J., Yan, M., 2014c. Electrochim. Acta 141, 391–397.
Li, W., Li, L., Ge, S., Song, X., Ge, L., Yan, M., Yu, J., 2013c. Chem. Commun. 49, 7687–7689.
Li, X., Ballerini, D.R., Shen, W., 2012. Biomicrofluidics 6, 011301–011313.
Li, L., Zhang, Y., Liu, F., Su, M., Liang, L., Ge, S., Yu, J., 2015. Chem. Commun. 51, 14030–14033.
Liu, H., Zhou, X., Liu, W., Yang, X., Xing, D., 2016. Anal. Chem. 88, 10191–10197.
Liu, H., Zhou, X., Shen, Q., Xing, D., 2018. Theranostics 8, 2289–2299.
Liu, W., Ma, C., Yang, H., Zhang, Y., Yan, M., Ge, S., Yu, J., Song, X., 2014. Microchim. Acta 181, 1415–1422.
Liu, X., Jiang, H., Lei, J., Ju, H., 2007. Anal. Chem. 79, 8055–8806.
Lo, S.-J., Yang, S.-C., Yao, D.-J., Chen, J.-H., Tu, W.-C., Cheng, C.-M., 2013. Lab Chip 13, 2686–2692.
Lu, J., Ge, S., Ge, L., Yan, M., Yu, J., 2012. Electrochim. Acta 80, 334–341.
Lutz, B., Liang, T., Fu, E., Ramachandran, S., Kauffman, P., Yager, P., 2013. Lab Chip 13, 2840–2847.
Maejima, K., Tomikawa, S., Suzuki, K., Citterio, D., 2013. RSC Adv. 3, 9258–9263.
Martinez, A.W., Phillips, S.T., Whitesides, G.M., Carrilho, E., 2010. Anal. Chem. 82, 3–10.
Miao, W., 2008. Chem. Rev 108, 2506–2553.
Mukhopadhyay, R., 2009. Anal. Chem. 81 (8659–8659).
Nie, Z., Nijhuis, C.A., Gong, J., Chen, X., Kumachev, A., Martinez, A.W., Narovlyansky, M., Whitesides, G.M., 2010. Lab Chip 10, 477–483.
Oh, Y.K., Joung, H.-A., Kim, S., Kim, M.-G., 2013. Lab Chip 13, 768–772.
Olkkonen, J., Lehtinen, K., Erho, T., 2010. Anal. Chem. 82, 10246–10250.
Ozcan, A., 2014. Lab Chip 14, 3187–3194.
Pedram, P., Mahani, M., Torkzadeh-Mahani, M., Hasani, Z., Ju, H.H., 2015. Microchim. Acta 183, 67–71.
Pei, X., Zhang, B., Tang, J., Liu, B., Lai, W., Tang, D., 2013. Anal. Chim. Acta 758, 1–18.
Ponomarenko, L.A., Schedin, F., Katsnelson, M.I., Yang, R., Hill, E.W., Novoselov, K.S., Geim, A.K., 2008. Science 320, 356–358.
Rizwan, M., Mohd-Naim, N.F., Ahmed, M.U., 2018. Sensors 18, 166. https://doi.org/10.3390/s18010166.
Richter, M., 2004. Chem. Rev. 104, 3003–3036.
Roda, A., Mirasoli, M., Michelini, E., Fusco, M.D., Zangheri, M., Cevenini, L., Roda, B., Simoni, P., 2016. Biosens. Bioelectron. 76, 164–179.
Roda, A., Guardigli, M., Calabria, D., Calabretta, M.M., Cevenini, L., Michelini, E., 2014. Analyst 139, 6494–6501.
Sardesai, N.P., Kadimisetty, K., Faria, R., Rusling, J.F., 2013. Anal. Bioanal. Chem. 405, 3831–3838.
Sher, M., Zhuang, R., Demirci, U., Asghar, W., 2017. Expert. Rev. Mol. Diagn. 17, 351–366.
Shi, C.-G., Shan, X., Pan, Z.-Q., Xu, J.-J., Lu, C., Bao, N., Gu, H.-Y., 2012. Anal. Chem. 84, 3033–3038.
Sia, S.K., Kricka, L.J., 2008. Lab Chip 8, 1982–1983.
Song, Y., Gyarmati, P., Araujo, A.C., Lundeberg, J., Brumer, H., Stahl, P.L., 2014. Anal. Chem. 86, 1575–1582.
Sun, H., Wu, L., Wei, W., Qu, X., 2013. Mater. Today 16, 433–442.
Sun, X., Li, B., Tian, C., Yu, F., Zhou, N., Zhan, Y., Chen, L., 2018. Anal. Chim. Acta 1007, 33–39.
Thom, N.K., Lewis, G.G., Yeung, K., Phillips, S.T., 2014. RSC Adv. 4, 1334–1340.
Valenti, G., Rampazzo, E., Bonacchi, S., Khajvand, T., Juris, R., Montalti, M., Marcaccio, M., Paolucci, F., Prodi, L., 2012. Chem. Commun. 48, 4187–4189.
Veigas, B., Jacob, J.M., Costa, M.N., Santos, D.S., Viveiros, M., Inacio, J., Martins, R., Barquinha, P., Fortunato, E., Baptista, P.V., 2012. Lab Chip 12, 4802–4808.
Wang, H.-K., Tsai, C.-H., Chen, K.-H., Tang, C.-T., Leou, J.-S., Li, P.-C., Tang, Y.-L., Hsieh, H.-J., Wu, H.-C., Cheng, C.-M., 2014a. Adv. Health Mater. 3, 187–196.
Wang, J., Monton, M.R.N., Zhang, X., Filipe, C.D.M., Pelton, R., Brennan, J.D., 2014b. Lab Chip 14, 691–695.
Wang, S., Dai, W., Ge, L., Yan, M., Yu, J., Song, X., Ge, S., Huang, J., 2012a. Chem. Commun. 48, 9971–9973.
Wang, S., Ge, L., Yan, M., Yu, J., Song, X., Ge, S., Huang, J., 2013. Sens. Actuators B: Chem. 176, 1–8.
Wang, S., Ge, L., Zhang, Y., Song, X., Li, N., Ge, S., Yu, J., 2012b. Lab Chip 12, 4489–4498.
Wang, X.H., Qu, K.G., Xu, B.L., Ren, J.S., Qu, X.G., 2011. J. Mater. Chem. 21, 2445–2450.
Wu, L., Ma, C., Ge, L., Kong, Q., Yan, M., Ge, S., Yu, J., 2015a. Biosens. Bioelectron. 63, 450–457.
Wu, L., Ma, C., Zheng, X., Liu, H., Yu, J., 2015b. Biosens. Bioelectron. 68 (413f), 314–420.
Wu, L., Zhang, Y., Wang, Y., Ge, S., Liu, H., Yan, M., Yu, J., 2016. Microchim. Acta 183, 1873–1880.
Xiao, Y., Rowe, A.A., Plaxco, K.W., 2007. J. Am. Chem. Soc. 129, 262–263.
Xu, C.X., Liu, Y.Q., Su, F., Liu, A.H., Qiu, H.J., 2011. Biosens. Bioelectron. 27, 160–166.
Xu, J., Huang, P., Qin, Y., Jiang, D., Chen, H.-Y., 2016. Anal. Chem. 88, 4609–4612.
Xu, J., Zhang, Y., Li, L., Kong, Q., Zhang, L., Ge, S., Yu, J., 2018. ACS Appl. Mater. Interfaces 10, 3431–3440.
Yager, P., Domingo, G.J., Gerdes, J., 2008. Annu. Rev. Biomed. Eng. 10, 107–144.
Yan, J., Yan, M., Ge, L., Ge, S., Yu, J., 2014. Sens. Actuators B: Chem. 193, 247–254.
Yan, J., Yan, M., Ge, L., Yu, J., Ge, S., Huang, J., 2013. Chem. Commun. 49, 1383–1385.
Yan, J., Ge, L., Song, X., Yan, M., Ge, S., Yu, J., 2012a. Chem. Eur. J. 18, 4938–4945.
Yan, M., Ge, L., Gao, W.Q., Song, X.R., Ge, S.G., Jia, Z.Y., Chu, C.C., Yu, J.H., 2012b. Adv. Funct. Mater. 22, 3899–3906.
Yang, H., Kong, Q., Wang, S., Xu, J., Bian, Z., Zheng, X., Ma, C., Ge, S., Yu, J., 2014a. Biosens. Bioelectron. 61, 21–27.
Yang, H., Kong, Q., Wang, S., Xu, J., Bian, Z., Zheng, X., Ma, C., Ge, S., Yu, J., 2014b. Biosens. Bioelectron. 61, 21–27.
Yang, H., Zhang, Y., Li, L., Zhang, L., Lan, F., Yu, J., 2017. Anal. Chem. 89 (14), 7511–7519.
Yeh, C.H., Chen, W.T., Lin, H.P., Chang, T.C., Lin, Y.C., 2009. Sens. Actuators B: Chem. 139, 387–393.
Yildiz, U.H., Alagappan, P., Liedberg, B., 2012. Anal. Chem. 85, 820–824.
Zhang, D., Liu, Q., 2016. Biosens. Bioelectron. 75, 273–284.
Zhang, L., Li, L., Ma, C., Ge, S., Yan, M., Bian, C., 2015. Sens Actuators B: Chem. 221, 799–806.
Zhang, M., Ge, L., Ge, S., Yan, M., Yu, J., Huang, J., Liu, S., 2013a. Biosens. Bioelectron. 41, 544–550.
Zhang, Q., Xiao, Q., Lin, Z., Ying, X., Li, Z., Lin, J.M., 2010. Clin. Biochem. 43, 1003–1008.
Zhang, X., Li, J., Chen, C., Lou, B., Zhang, L., Wang, E., 2013b. Chem. Commun. 49, 3866–3868.
Zhang, Y., Li, L., Yang, H., Ding, Y., Su, M., Zhu, J., Yan, M., Yu, J., Song, X., 2013c. RSC Adv. 3, 14701–14709.
Zheng, L.Y., Chi, Y.W., Dong, Y.Q., Lin, J.P., Wang, B.B., 2009. J. Am. Chem. Soc. 131, 4564–4565.
Zhou, J., Gan, N., Li, T., Zhou, H., Li, X., Cao, Y., Wang, L., Sang, W., Hu, F., 2013. Sens. Actuators B: Chem. 178, 494–500.
Zhou, Y., Yan, D., Wei, M., 2015. J. Mater. Chem. C 3, 10099–10106.